Technical note

Study for electron ionisation process and models in Geant4

Summary

Up to Geant4 10.6 version (2021), Livermore electron photon models were based on three evaluated data libraries of the Lawrence Livermore National Laboratory (LLNL) for elements with atomic number Z: 1–100, designed in the 1990′ s. These libraries have undergone a major updating process under the auspices of the International Atomic Energy Agency (IAEA), resulting in a new version, EPICS2017 (Electron-Photon Interaction Cross Sections). This technical note describes a supplementary study in the frame of the PhD thesis [1] "Implementation of the EPICS2017 electron-photon database in Geant4: developments and applications", which was meant to implement EPICS2017 to Livermore models. More specifically, for electrons, the possible update of the ionisation and excitation model was considered.

By comparing EPICS2017 to previous version, we noted that the cross-sections exhibit differences only at low energy, due to the modifications of binding energies of outer subshells. Furthermore, we compared the calculated cross-sections and stopping powers obtained from the existing Livermore model, in order to determine whether updating the model with EPICS2017 is necessary. The results did not show significant difference. Consequently, it was concluded that the implementation of EPICS2017 for electrons is not required. This was actually expected, quoting Dr Cullen [2]: "*Updating the binding energies is important so that the EPICS2017 data reproduce the well-known characteristic fluorescence X-rays, as shown in Deslattes paper [3], but based on the small shifts in the electron ionization data, shown below, we should not expect much of a change in the transport and slowing down of electrons*".

Introduction

This technical note describes a study for electron ionisation process and models in Geant4, including Livermore, Penelope and MollerBhabha models. More specifically for Livermore, it is based on EEPDL91 database.

For this, we first show in section 1 the data format in EPICS2017 and in section 2 the main changes that would possibly have impact on Livermore models, *i.e.*, ionisation cross-section. In section 3, we explain how Livermore model calculates cross-section and stopping power, which are two fundamental physical quantities used in the modelling of ionisation process. In section 4, we show the comparison of cross-section and stopping power calculated by Livermore model of Geant4 10.7 and EEDL91, EEDL2017 (EPICS2017) databases.

The second objective of this technical note is to show the comparison of the cross-section and stopping power calculated by Livermore, Penelope and MollerBhabha models in section 5. Furthermore, the stopping powers from other data sources, such as NIST and ICRU90 are considered in the comparison in section 6.

In section 7, we provide a list of the scripts used for this study.

1. Description of EPICS2017 electron data

1.1. General presentation

EPICS2017 [4] is the Electron Photon Interaction Cross Section library that provides the atomic data needed to perform Electron and Photon transport calculations. Atomic data are provided for elements Z: 1-100, over the energy range 10 eV to 100 GeV. EPICS2017 includes three sub-libraries:

- EEDL [2]: the Evaluated Electron Data Library, describes the interaction of electrons with matter
- EPDL [5]: the Evaluated Photon Data Library, describes the interaction of photons with matter
- EADL [6]: the Evaluated Atomic Data Library, describes the emission of electrons and photons following an ionizing event, caused by either electron or photon interaction on atoms

EPICS2017 can be downloaded via *https://www-nds.iaea.org/epics/*

Two formats are available: ENDF and ENDL. For our study, we used the ENDL format.

1.2. Physical quantities

In EPICS2017, the sub-library that describes the interaction of electrons with matter is the Evaluated Electron Data Library (EEDL2017). It provides complete information for particle transport covering elements Z: 1-100 and incident electron energies ranging from 10 eV to 100 GeV. The physical quantities available in the database are as follows:

i) Elastic transport

- Transport cross section (barn).

ii) Large angle elastic scattering

- Integrated large angle scattering cross section (barn);
- Average energy of the scattered electron (MeV);
- Average energy to the residual atom, *i.e.*, local deposition (MeV);
- Angular distribution of the scattered electron.

iii) Elastic scattering

- Integrated scattering cross section (barn).

iv) Ionisation

- Integrated **total** cross section (barn);

- Integrated **subshell** cross section (barn);
- Average energy of the scattered electron (MeV) by subshell;
- Average energy of the recoil electron (MeV) by subshell;
- Spectra of the recoil electron.

v) Bremsstrahlung

- Integrated cross section (barn);
- Average energy of the secondary electron and positron (MeV);
- Average energy of the secondary positron (MeV);
- Spectra of the secondary photon.

vi) Excitation

- Integrated cross section (barn);
- Average energy to the residual atom, *i.e.*, local deposition (MeV).

1.3. Format of data

1.3.1. Structure of data

Similar to EPDL2017 in EPICS2017, EEDL2017 contains a series of tables in **ASCII format**. Each table starts with **two header lines** that contain the parameters related to the physical data (Figure 1). These two header lines are followed by a series of two (or three)-column **physical data lines**, one data point per line. Each table is terminated by an end of table line which is blank except for a "1" placed in column 72 (column 72 is blank on all other lines in the table).

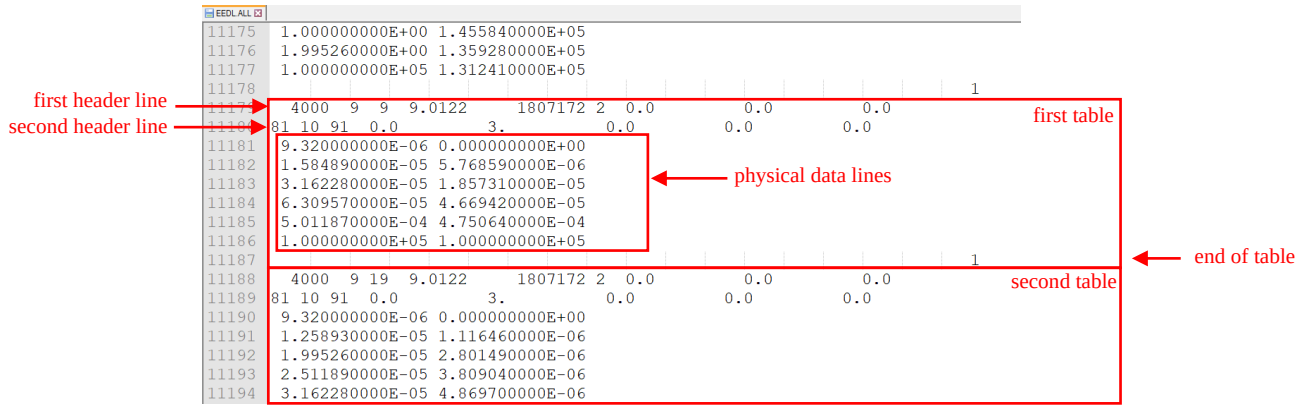

Figure 1. Example of two tables contained in EEDL2017. Header lines, end of table line and physical data lines are indicated (red arrows).

1.3.2. Information in the first header line

As an example, some detailed explanations are given in Figure 2 for the first header line, extracted from the first table presented in Figure 1.

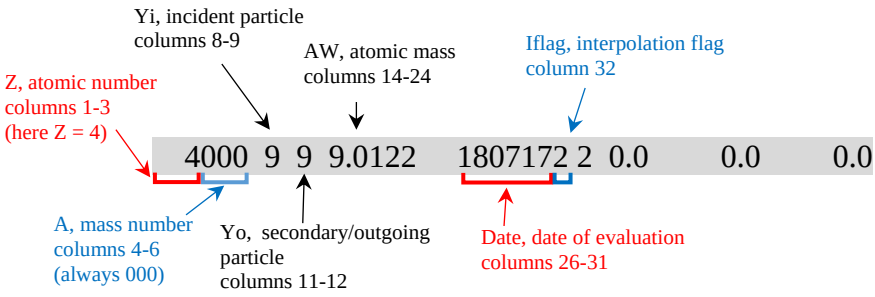

Figure 2. Information in the first header line of a table.

Additional information:

- For mass number, in all cases A = 0 (for elemental data)
- For **incident** particle (**i index**):
  - Yi = 9, electron
- For secondary/**outgoing** particle (**o index**):
  - Yo = 0, no secondary/outgoing particle
  - Yo = 7, photon
  - Yo = 9, electron
  - Yo = 19, electron as recoil
- For date: YYMMDD
- For interpolation flag:
  - Iflag = 0, or 2, linear in x and y
  - Iflag = 3, logarithmic in x, linear in y
  - Iflag = 4, linear in x, logarithmic in y
  - Iflag = 5, logarithmic in x and y

1.3.3. Information in the second header line

Figure 3 illustrates the information contained in the second header line, extracted from the first table presented in **Erreur ! Source du renvoi introuvable.**.

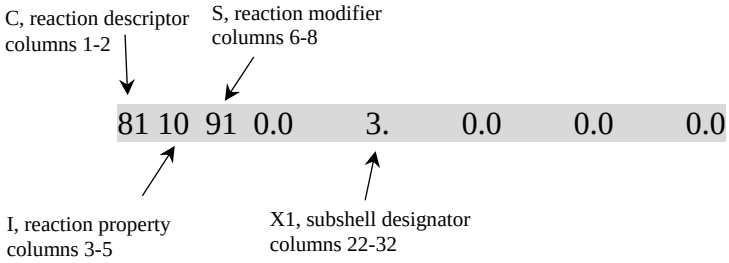

Figure 3. Information in the second line of a table.

Additional information:

- For reaction descriptor (it is equivalent to the notion “physical process” used in Geant4):

    - C = 7, elastic transport
    - C = 8, large angle elastic scattering
    - C = 10, elastic scattering
    - C = 81, ionisation
    - C = 82, bremsstrahlung
    - C = 83, excitation
- For reaction property:
    - I = 0, integrated cross section
    - I = 10, average energy of the secondary particle, Yo
    - I = 11, average energy to the residual atom
    - I = 21, spectra of recoil particle
    - I = 22, angular distribution
- For reaction modifier:
    - S = 0, no X1 field data required
    - S = 91, X1 field data required
- For X1, value depends upon the value of S:
    - S = 0, X1 = 0
    - S = 91, X1 = subshell designator, as shown in Table 1

Table 1: Atomic subshells in EPICS2017 are specified by prescribed floating point designators.

Designator	Subshell	Designator	Subshell	Designator	Subshell
1	K (1s1/2)	21	N4 (4d3/2)	41	P1 (6s1/2)
2	L (2)	22	N5 (4d5/2)	42	P23 (6p)
3	L1 (2s1/2)	23	N67 (4f)	43	P2 (6p1/2)
4	L23 (2p)	24	N6 (4f5/2)	44	P3 (6p3/2)
5	L2 (2p1/2)	25	N7 (4f7/2)	45	P45 (6d)
6	L3 (2p3/2)	26	O (5)	46	P4 (6d3/2)
7	M (3)	27	O1 (5s1/2)	47	P5 (6d5/2)
8	M1 (3s1/2)	28	O23 (5p)	48	P67 (6f)
9	M23 (3p)	29	O2 (5p1/2)	49	P6 (6f5/2)
10	M2 (3p1/2)	30	O3 (5p3/2)	50	P7 (6f7/2)
11	M3 (3p3/2)	31	O45 (5d)	51	P89 (6g)
12	M45 (3d)	32	O4 (5d3/2)	52	P8 (6g7/2)
13	M4 (3d3/2)	33	O5 (5d5/2)	53	P9 (6g9/2)
14	M5 (3d5/2)	34	O67 (5f)	54	P1011 (6h)
15	N (4)	35	O6 (5f5/2)	55	P10 (6h9/2)
16	N1 (4s1/2)	36	O7 (5f7/2)	56	P11 (6h11/2)
17	N23 (4p)	37	O89 (5g)	57	Q (7)
18	N2 (4p1/2)	38	O8 (5g7/2)	58	Q1 (7s1/2)
19	N3 (4p3/2)	39	O9 (5g9/2)	59	Q23 (7p)
20	N45 (4d)	40	P (6)	60	Q2 (7p1/2)
				61	Q3 (7p3/2)

1.3.4. Physical data lines

Following the two header lines, the two (or three)-column physical data lines are provided with 10 significant digits. The physical quantities tabulated in these data lines depend on the value of the reaction descriptor and property, which are indicated in the second header line (Figure 3).

1.4. Main changes

A fundamental modification of EPICS2017 is the change in binding energies, which have been updated to electron data in EEDL2017. This update results in changes in related physical quantities, such as the ionisation and excitation cross-sections. On the opposite, some physical quantities, such as bremsstrahlung cross-sections, are not affected as they are independent of the binding energies.

2. Comparison of ionisation cross-section between EEDL2017 and EEDL2014 (EEDL91)

In this section, we carried out the comparison of ionisation and excitation cross-sections between EEDL2017 and previous version to see if there is some difference. The previous EEDL database that we used is the version of 2014. It is worthwhile to point out there is no difference in the data values between the version 2014 and the version 91. The only difference lies in the format. Data in EEDL2014 are in a simple computer independent text format that can be easily read by computer codes, while data in EEDL91 are not. (The power of 10 is written differently).

The comparison is performed in terms of both subshell cross-section and total cross-section in section 2.1 and 2.2 respectively.

Need to point out here that there are many plots in this technical note, we use the naming EEDL2017 to represent the EPICS2017 electron data in the legends of plots. EEDL2014 for EPICS2014.

2.1. Comparison of subshell ionisation cross-section

There are 1612 subshells in total for 100 elements (Z: 1-100). The modification of binding energies in EEDL2017 leads to an energy shift near the binding energy for each subshell [6]. An example is given here for iron, between EEDL2017 and EEDL2014 (Figure 4). More specifically, the shift only occurs in the vicinity of the binding energy, as depicted in Figure 5, which shows a part of the tabulated data for this subshell. The shift in energy is visible: the subshell cross-section values keep unchanged (in blue), while only energies near the binding energy point are different (in red). This phenomenon is stated in the survey of Dr. Cullen [2]**.** We quote here: "*After reviewing all the electron data, I have decided for EPICS2017 that it is sufficient to only change binding energies, to ensure they are consistent with the changes already made to EADL and EPDL*".

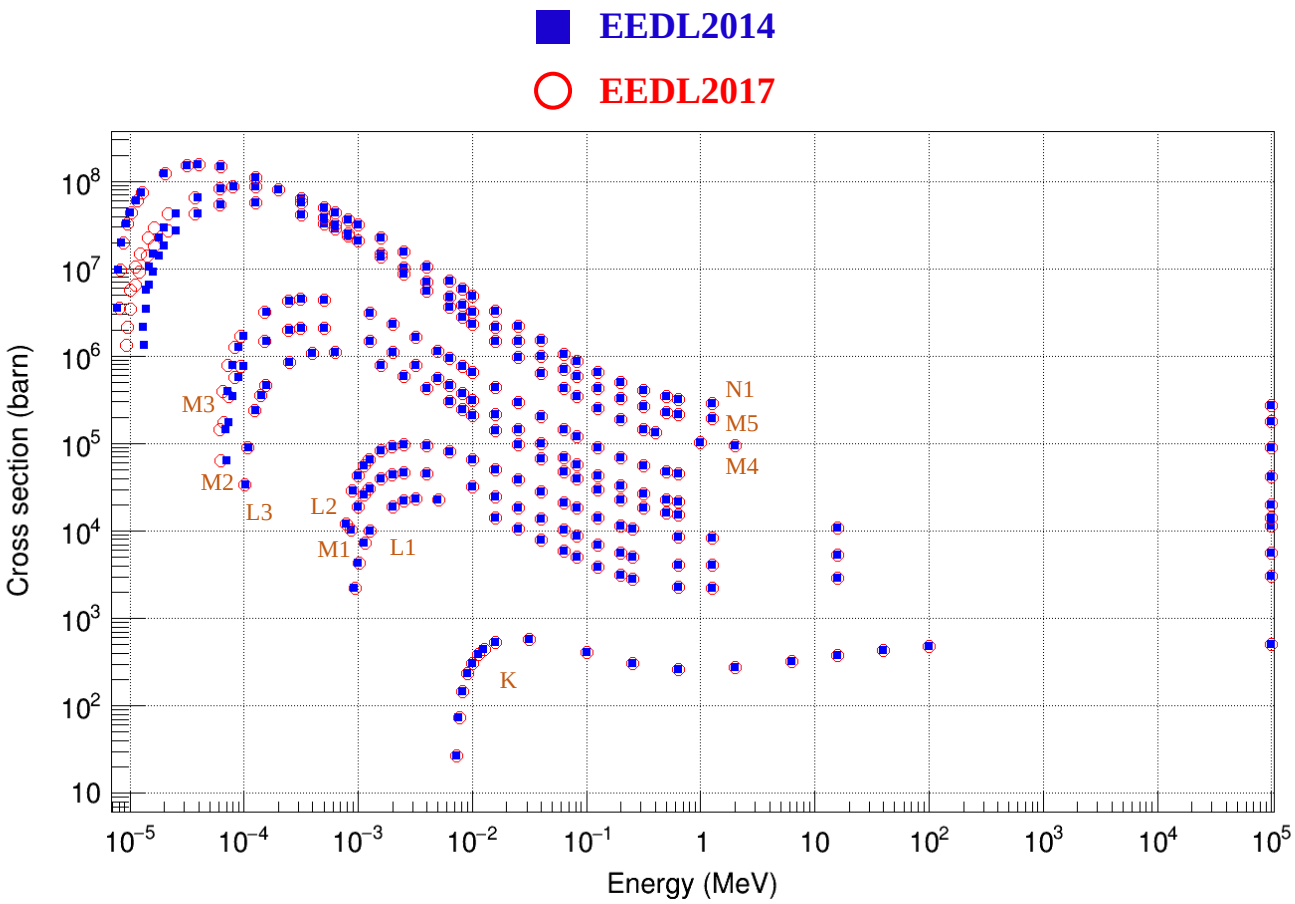

Figure 4. Subshell cross-sections comparison between EEDL2017 and EEDL91 for iron. The first tabulated point for each subshell corresponds to the binding energy (first point in Figure 5); the cross-section value at this point is 0, so this point is not plotted.

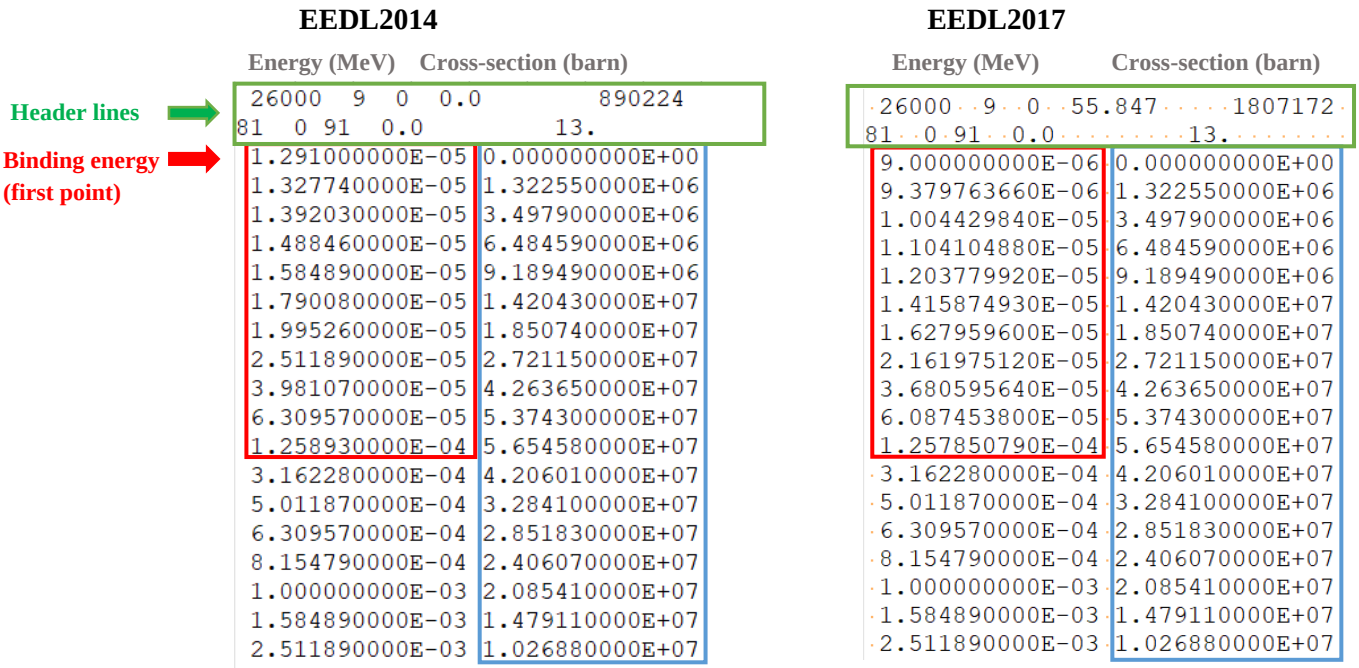

Figure 5. Beginning of the subshell cross-section data in EEDL2014 and EEDL2017 for the M4 subshell of iron.

2.2. Comparisons of total ionisation cross-sections

In EEDL2014, the total ionisation cross-sections are not available, whereas they are included in EEDL2017. They are calculated by summing up the subshell cross-sections using the appropriate interpolation, *i.e.*, logarithmic interpolation for EEDL2014 and linear interpolation for EEDL2017. Figure 6 shows an example of total cross-sections for hydrogen (H), iron (Fe), and lead (Pb). The bottom graph displays the relative difference (*RD*), expressed as follows:

$$RD\ (\%) = 100 \times \frac{EEDL2017 - EEDL91}{EEDL91} \qquad (1)$$

As expected, we observed large differences at low energies, which correspond to the energy shift observed for the outer subshells (section 2.1 of this chapter).

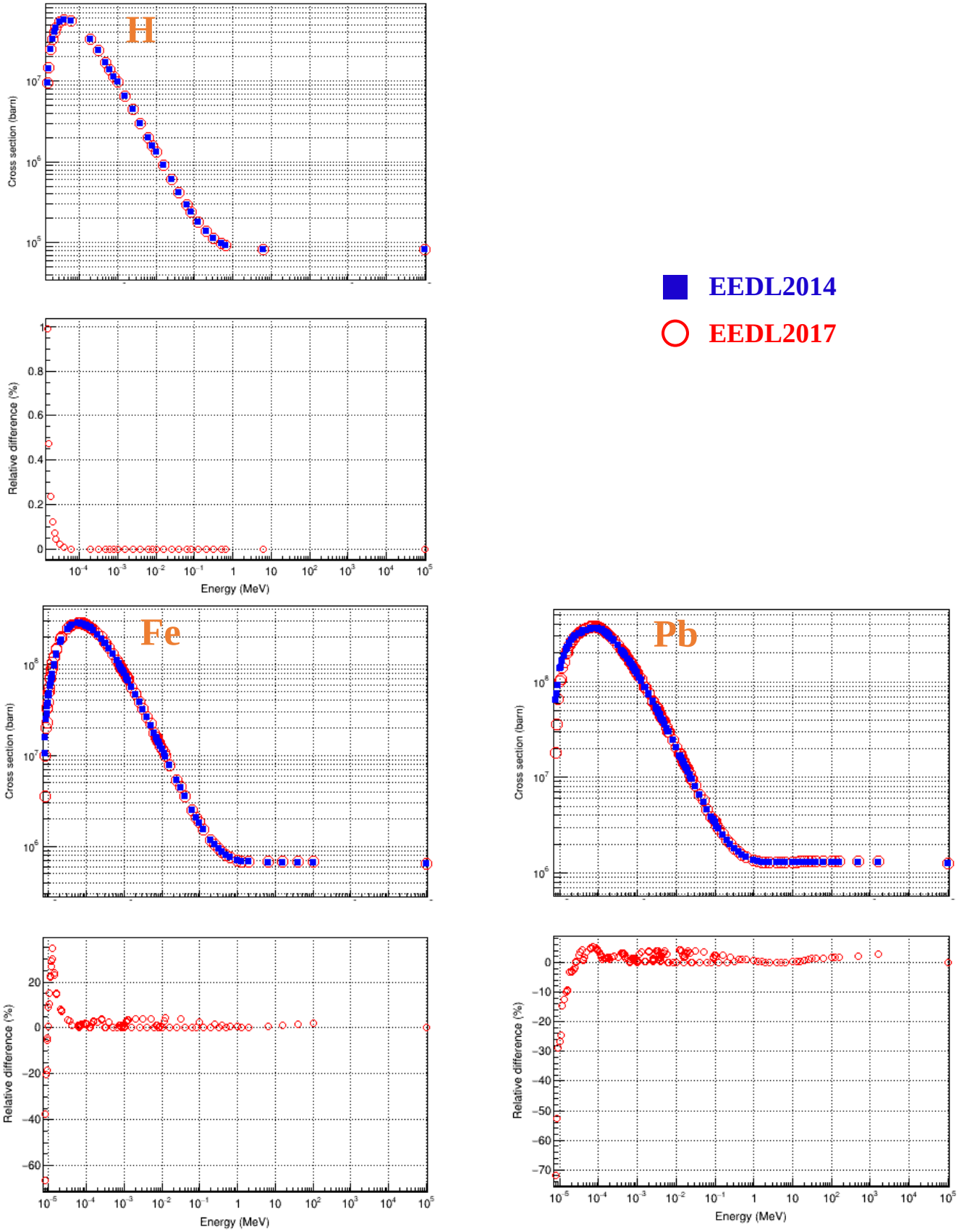

Figure 6. Comparison of total ionisation cross-section for H, Fe and Pb between EEDL2017 and EEDL91. The relative difference (RD) of EEDL2017 compared to EEDL91 is calculated according to equation (1). The energy scale is the same for both cross-sections and RD.

3. Livermore ionisation model in Geant4

The objective of this section is to introduce the Livermore ionisation model and explain its calculation process of cross-section and stopping power.

3.1. Ionisation process in Geant4

The ionisation process occurs when an incident electron interacts with orbital electrons, leading to the generation of a secondary electron. In the simulation, Geant4 imposes a parameter called production cut T_{cut} for secondary particles, which corresponds to the minimum energy of a secondary electron that can be generated by an interaction [7]. Indeed, T_{cut} is used to control the level of detail in the simulation, aiming to improve the computational efficiency by excluding low-energy secondary particles that may not significantly impact the final results.

In Geant4, the ionisation process is handled by the ***G4eIonisation*** class, which has discrete and continuous components [7, 8]:

- If the discrete interaction is invoked, a secondary electron with energy t above T_{cut} is explicitly generated. The probability of this interaction is determined by the ***restricted*** cross-section (section 3.2);
- In the continuous interaction, the mean energy loss per unit length, also known as the stopping power, is calculated by the ***restricted*** stopping power along the step (section 3.3).

The combination of continuous and discrete interactions in Geant4 enables accurate simulation of the behavior of electrons as they interact with matter. More precisely, the total energy loss ΔE of incident electron during an interaction step due to ionisation is calculated as follows:

$$\Delta E = \Delta E_{continuous} + \Delta E_{discrete} \qquad (2)$$

where:

- $\Delta E_{continuous}$ is the ***restricted*** energy loss calculated from continuous interaction, which is considered as energy deposited locally;
- $\Delta E_{discrete}$ is the energy loss during the discrete interaction, if invoked.

In Geant4, an ionisation model performs two major tasks:

- Computation of cross-section, to determine the probability of an electron undergoing ionisation interaction as it passes through a material. It is performed by the ***ComputeCrossSectionPerAtom()*** method;
- Sampling of the final state after an interaction, performed by the ***SampleSecondaries()*** method. This method is called to generate the final state of the incident electron after a step interaction, such as its energy and momentum. It also simulates the generation of the secondary particle(s) produced as a result of the interaction.

In the following sections 3.2 and 3.3., we will introduce more precisely the calculation of cross-section and stopping power using by ***G4LivermoreIonisationModel***.

3.2. Calculation of ionisation cross-section

When a discrete interaction is invoked, the secondary electron with energy ***above*** T_{cut} is explicitly simulated through a discrete interaction. The probability of this interaction is determined by the ***restricted*** cross-section $\sigma(E, T_{cut})$, which is calculated by Livermore ionisation model as follows [8, 9]:

$$\sigma(E, T_{cut}) = \int_{T_{cut}}^{T_{max}} \frac{d\sigma(E,t)}{dt} dt = \sum_{s=0}^{n-1} \left(\sigma_s(E) \frac{\int_{T_{cut}}^{T_{max}} \frac{d\sigma}{dt} dt}{\int_{0.1eV}^{T_{max}} \frac{d\sigma}{dt} dt} \right) \qquad (3)$$

where:

- t is the kinetic energy of secondary electron;
- E is the energy of incident electron;
- $\frac{d\sigma}{dt}$ is the distribution of cross-sections as a function of the kinetic energy t of the secondary electron. ***It is calculated through a parameterization of the energy spectrum data in EEDL***;
- $T_{max} = 0.5E$ is the maximum energy transferred to a secondary electron;
- $\sigma_s(E)$ is the subshell cross-section obtained from an interpolation of the tabulated cross-section data in EEDL, ***and 0.1 eV is the low energy limit of secondary electron in EEDL***;
- s is the considered subshell;
- n is the total number of subshells.

During a Geant4 simulation, the ***restricted*** cross-section $\sigma(E, T_{cut})$ for a given energy of incident electron E and production T_{cut} is obtained using the ***ComputeCrossSectionPerAtom()*** method implemented in ***G4LivermoreIonisationModel***.

3.3. Calculation of continuous energy loss

Whatever the case, the discrete interaction being invoked or not, the continuous interaction is always simulated, in which the restricted energy loss below T_{cut}, is calculated. The ***restricted*** energy loss is obtained by multiplying the interaction step length by the ***restricted*** stopping power. In Livermore model, the ***restricted*** stopping power due to ionisation [8, 9] is expressed via the sum over all atomic subshells s and the integral over the energy t of secondary electron:

$$-\frac{dE(E, T_{cut})}{dx} = n_{at} \int_0^{T_{lim}} \frac{d\sigma(E,t)}{dt} t dt = n_{at} \sum_{s=0}^{n-1} (\sigma_s(E) \frac{\int_{0.1eV}^{T_{lim}} \frac{d\sigma}{dt} t dt}{\int_{0.1eV}^{T_{max}} \frac{d\sigma}{dt} dt}) \qquad (4)$$

where:

- E is the energy of incident electron;
- $T_{lim} = \min(T_{cut}, T_{max})$ is the maximal energy transferred during a continuous interaction;

- n_{at} is the number of atoms per unit volume in the material.

Here the ***restricted*** cross-section $\frac{d\sigma}{dt}$ is calculated using the same parameterization of the energy spectra as mentioned in section 3.2. The calculation of ***restricted*** stopping power at a given energy can be retrieved using the ***ComputeDEDXPerVolume()*** method in ***G4LivermoreIonisationModel***. However, it should be noted that the value returned by ***ComputeDEDXPerVolume()*** is not the ***restricted*** stopping power only due to ionisation. Actually it is the ***restricted collision stopping power***, which is the energy loss per unit length induced by ***both ionisation and excitation***. Contrary to the ionisation process, the excitation is not explicitly modelled, but its contribution to the energy loss, which does not depend on T_{cut}, is directly included in the ionisation model.

4. Comparison of ionisation cross-section and stopping power between Livermore model and EEDL

The objective of this section is to compare cross-sections and stopping powers calculated from the existing Livermore ionisation model with those corresponding to EEDL2017 and EEDL91. More precisely, based on TestEm0 example, 73 energy points were chosen, ranging from 10 eV to 1 GeV, with 10 points evenly spaced in log scale for each energy interval: 10 eV - 100 eV; 100 eV - 1 keV; …; 100 MeV - 1 GeV. The following methods in the ***G4LivermoreIonisationModel*** are used to obtain the cross-sections and stopping powers at these energies:

- ***ComputeCrossSectionPerAtom()*** to calculate the cross-section;
- ***ComputeDEDXPerVolume()*** to calculate the collision stopping power.

4.1. Cross-section

As described in equation (3), the ***ComputeCrossSectionPerAtom()*** calculates the cross-section of generating a secondary electron with energy ***above*** T_{cut}. For this reason, to obtain the total ionisation cross-section, T_{cut} should be 0. However, as the minimal energy of secondary electron considered in EEDL is 0.1 eV, in practice we took T_{cut}= 0.1 eV instead of 0 for the calculation. We checked that the results, as expected, keep unchanged if we took values of T_{cut} below 0.1 eV. Figure 7 shows the ionisation cross-section comparisons for H, Fe and Pb taken as examples. The bottom graph shows the relative difference (*RD*) of EEDL91 and EEDL2017 cross-sections, compared to Livermore:

$$RD\ (\%) = 100 \times \frac{EEDL - Livermore}{Livermore} \qquad (5)$$

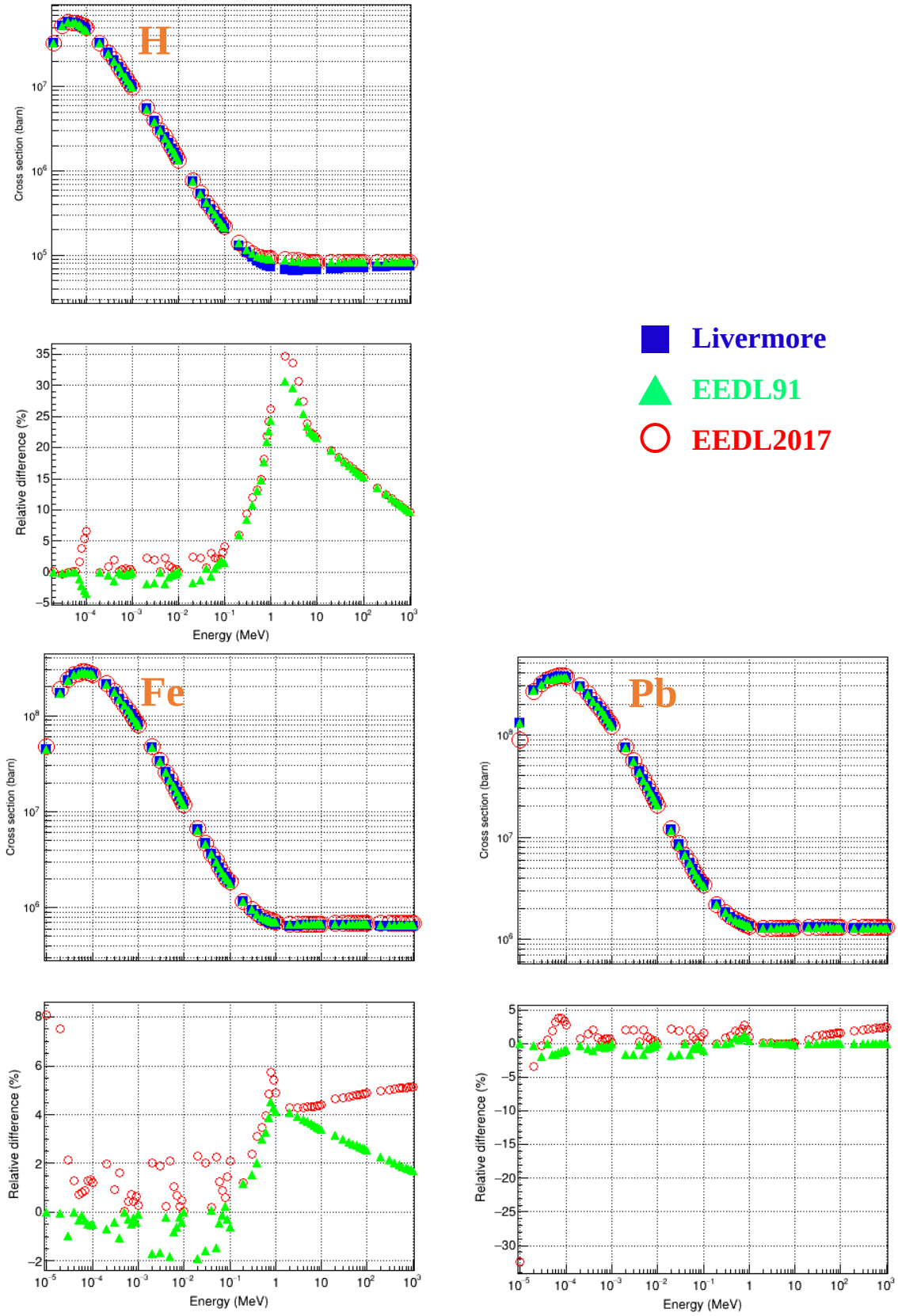

Figure 7. Ionisation cross-section of EEDL2017, EEDL91 and those calculated from the existing Livermore model, for H, Fe and Pb. The relative difference (RD) of EEDL2017 compared to EEDL91 is calculated according to equation (5). The energy scale is the same for both cross-sections and RD.

As explained in section 3.2, the calculation of cross-section by the existing Livermore ionisation model is via a parameterization based on EEDL91. We can see that the calculated cross-sections by Livermore model are also in agreement with EEDL2017. The corresponding relative difference values (red circles) are similar to those obtained with EEDL91 (green triangles), except in a very narrow region at low energy, which corresponds to the energy shift observed for the outer subshells, as shown in section 2.1. For this reason, we can conclude that updating the Livermore model is unnecessary regarding cross-sections.

4.2. Stopping power

4.2.1. EPICSHOW

EEDL2017 and EEDL91 do not contain stopping power data. However, Dr. Cullen has kindly and generously provided us with the EPICSHOW (Electron Photon Interactive Code - Show Data) program (Figure 8) (*https://inis.iaea.org/collection/NCLCollectionStore/_Public/30/022/30022812.pdf?r=1*), which can be used to compute and plot the stopping power corresponding to EEDL2017. It provides ionisation, bremsstrahlung, excitation and total stopping powers. To make a plot, we can simply choose the appropriate buttons: “Electrons”+ “Deposit” + “Blk/White”.

Figure 8. Interface of EPICSHOW program.

An example of the stopping power of H obtained from EPICSHOW is given in Figure 9. EPICSHOW can also produce data in text format for plots by using the “Listing” button if needed (Figure 10). We used the text format data to make the comparative study in section 4.3.4.

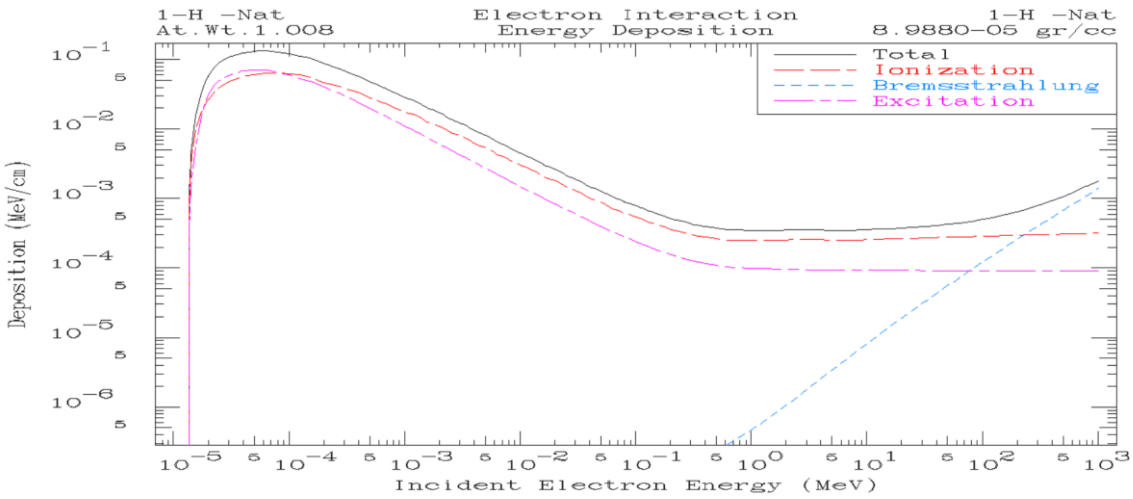

Figure 9. Stopping power of H calculated by EPICSHOW corresponding to EEDL2017 data.

Atomic Weight 1.008 — 1-H -Nat — 8.9880-05 grams/cc

Electron - Derived Quantities

Energy MeV	Total Cross Section barns	Mean Free Path 1/cm	Range cm	Energy Deposit (Mev/cm) cm*cm/gr	cm	Total	Ionize	Brems.	Excite
1.0000-05	2.7490+08	1.4761+04	6.7744-05	1.6423+08		3.4293-09		3.4293-09	
1.2500-05	2.2053+08	1.1842+04	8.4446-05	1.3175+08		4.2219-09		4.2219-09	
1.2589-05	2.1859+08	1.1738+04	8.5195-05	1.3059+08		4.2512-09		4.2512-09	
1.3610-05	2.0457+08	1.0985+04	9.1034-05	1.2222+08		4.5865-09		4.5865-09	
1.3784-05	2.0406+08	1.0958+04	9.1260-05	1.2191+08		1.3887-03	9.3047-04	4.6436-09	4.5823-04
1.4088-05	2.0316+08	1.0909+04	9.1667-05	1.2137+08		3.8084-03	2.5561-03	4.7435-09	1.2523-03
1.4170-05	2.0291+08	1.0896+04	9.1778-05	1.2123+08		4.4558-03	2.9931-03	4.7703-09	1.4627-03
1.5000-05	1.9978+08	1.0728+04	9.3218-05	1.1935+08		1.0719-02	7.1361-03	5.0428-09	3.5826-03
1.5009-05	1.9976+08	1.0727+04	9.3227-05	1.1934+08		1.0796-02	7.1826-03	5.0460-09	3.6136-03
1.5625-05	1.9760+08	1.0611+04	9.4243-05	1.1806+08		1.5695-02	1.0027-02	5.2482-09	5.6679-03
1.6000-05	1.9749+08	1.0604+04	9.4300-05	1.1799+08		1.9034-02	1.1659-02	5.3714-09	7.3751-03
1.7500-05	2.0164+08	1.0827+04	9.2357-05	1.2047+08		3.2918-02	1.7779-02	5.8838-09	1.5140-02
1.8359-05	2.0463+08	1.0988+04	9.1007-05	1.2225+08		4.1544-02	2.0987-02	6.1776-09	2.0557-02
1.9953-05	2.0904+08	1.1225+04	8.9086-05	1.2489+08		5.7141-02	2.6464-02	6.7222-09	3.0678-02
2.0000-05	2.0928+08	1.1238+04	8.8985-05	1.2503+08		5.7572-02	2.6594-02	6.7382-09	3.0978-02
2.0736-05	2.1144+08	1.1354+04	8.8078-05	1.2632+08		6.3217-02	2.8668-02	7.0010-09	3.4550-02
2.2500-05	2.1658+08	1.1630+04	8.5984-05	1.2939+08		7.6748-02	3.3640-02	7.5337-09	4.3108-02
2.2536-05	2.1660+08	1.1631+04	8.5977-05	1.2941+08		7.6951-02	3.3740-02	7.5446-09	4.3211-02
2.5000-05	2.1555+08	1.1575+04	8.6397-05	1.2878+08		8.9650-02	3.9420-02	8.2889-09	5.0230-02
2.6250-05	2.1524+08	1.1558+04	8.6520-05	1.2859+08		9.4459-02	4.1533-02	8.6760-09	5.2926-02
3.1623-05	2.1059+08	1.1308+04	8.8433-05	1.2581+08		1.1133-01	5.0238-02	1.0340-08	6.1093-02
3.2000-05	2.1030+08	1.1292+04	8.8555-05	1.2564+08		1.1209-01	5.0573-02	1.0456-08	6.1521-02

Figure 10. Part of the text data file for stopping power of H produced by EPICSHOW. The unit for stopping power is MeV/cm.

4.2.2. Comparison between EEDL91 and EEDL2017

In this section, we show the stopping power comaprison between EEDL2017 and EEDL91. Due to the lack of raw data for EEDL91, we only made a rough comparison by superposing the EEDL2017 graph on EEDL91 graph, which is available in the previous documentation [10]. So these comparisons were only made for indicative purpose. An example of EEDL91 stopping power graph is shown in Figure 11. It contains the contribution of three processes: ionisation, bremsstrahlung and excitation. The sum is

indicated as “total”. For elements from carbon, the fluorescence stopping power is also shown, which refers to the component of the ionisation that yields X-rays.

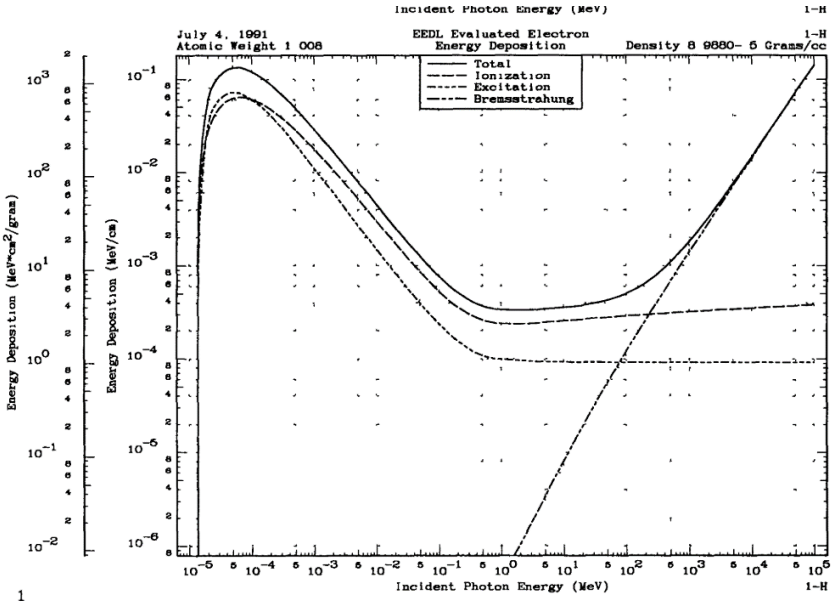

Figure 11. Stopping power for H in EEDL91.

These rough comparisons did not show major differences between EEDL2017 and EEDL91 (Figure 12). This was expected because, as mentioned in section 2.1, there is little change in the cross-sections, only small shifts in binding energies. This comparison also confirms the statement by Dr Cullen, we quote here: “*Updating the binding energies is important so that the EPICS2017 data reproduce the well-known characteristic fluorescence X-rays, as shown in Deslattes paper [3], but based on the small shifts in the electron ionization data, shown below, we should not expect much of a change in the transport and slowing down of electrons*”.

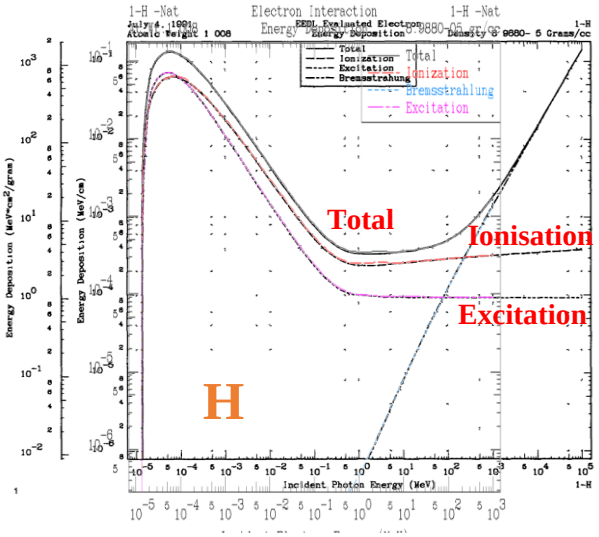
Total
Ionisation
Excitation
H

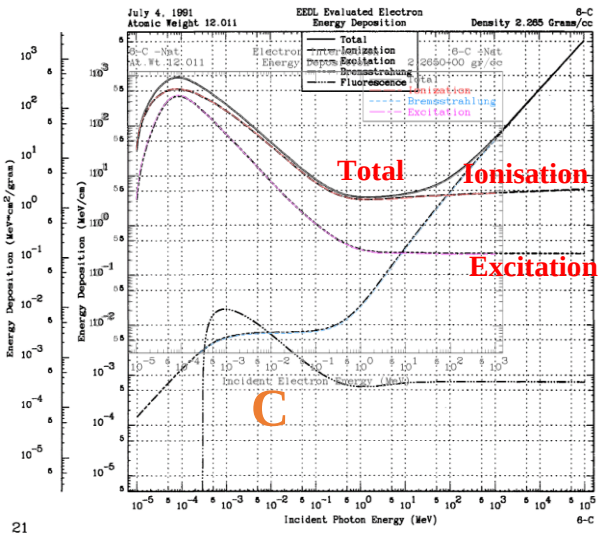
Total
Ionisation
Excitation
C

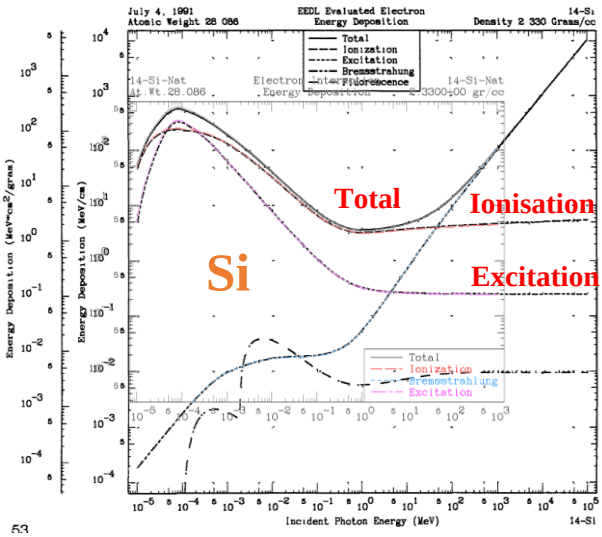
Total
Ionisation
Excitation
Si

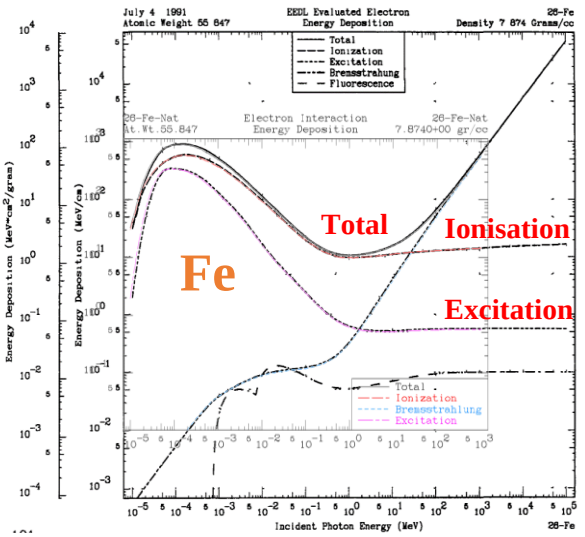
Total
Ionisation
Excitation
Fe

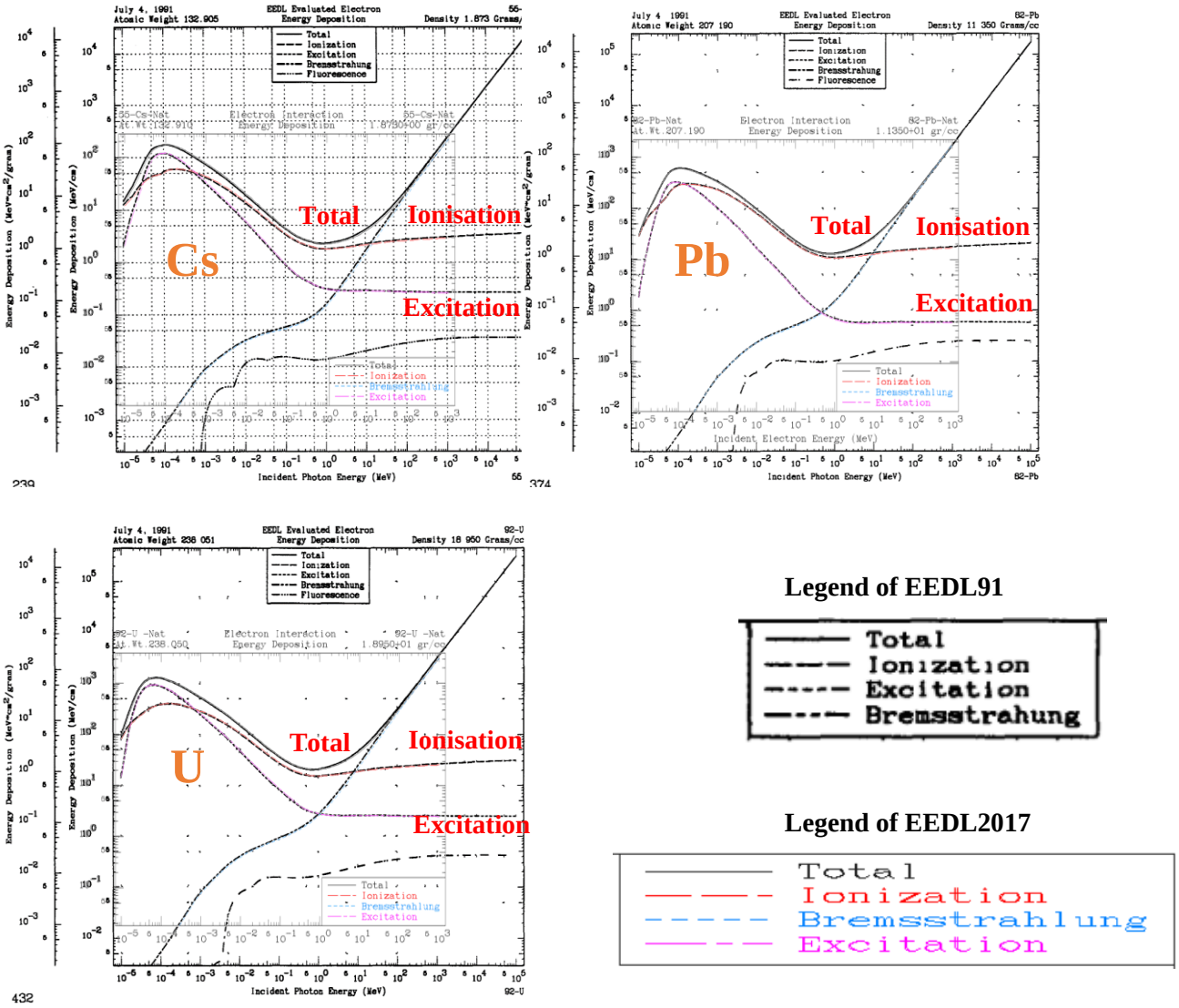

Figure 12. Comparison of stopping power for H, C, Si, Fe, Cs, Pb and U, between EEDL91 and EEDL2017.

4.2.3. Comparison between Livermore and EEDL2017

a) Collision stopping power

As explained in section 3.3, the ***ComputeDEDXPerVolume()*** method calculates the ***restricted*** collision stopping power induced by both ionisation and excitation. To obtain the total collision stopping power, T_{cut} should be larger than the highest transferred energy. In our comparison, the energy of incident electron ranges from E=10 eV-1 GeV. So in this case, $T_{max} = 0.5E = 0.5$ GeV. We took T_{cut}=10 GeV, but we have checked that the results, as expected, keep unchanged if we took values of T_{cut} above 0.5 GeV. Figure 13 shows the comparison between the stopping power obtained from EEDL2017 (EPICSHOW) and from the existing Livermore model, based on EEDL91. The relative differences observed are generally within a few percent. As the collision stopping power is the sum of excitation and ionisation, it is important to study separately the contribution of each process.

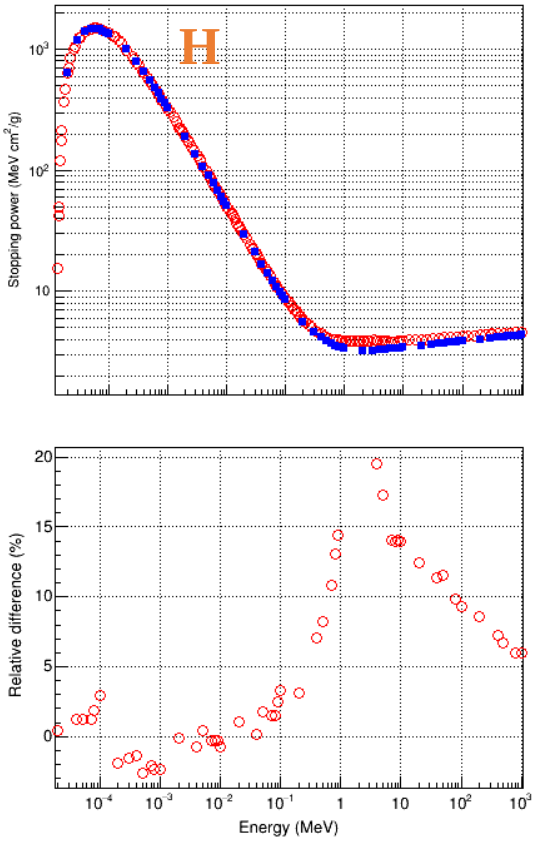

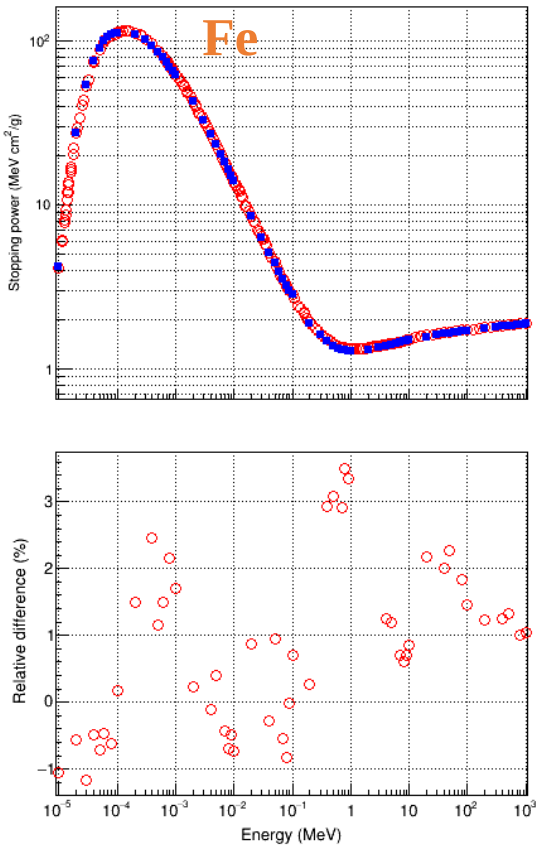

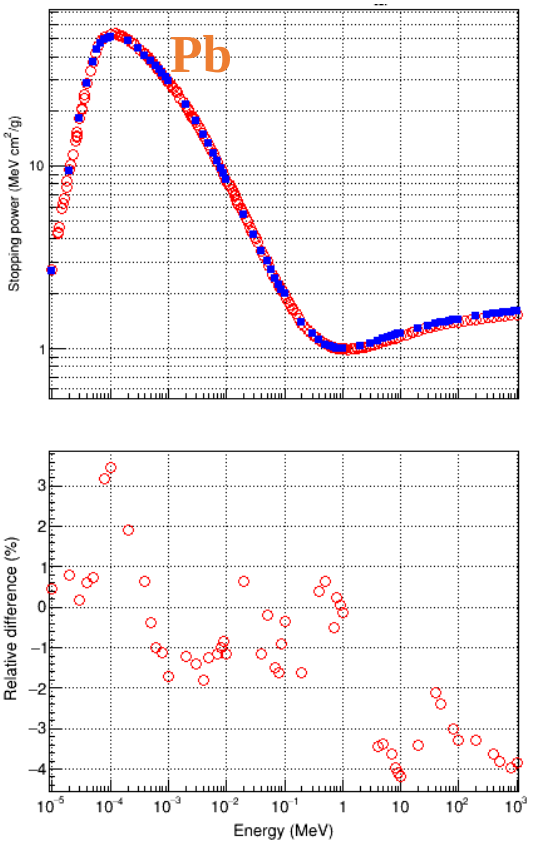

Livermore

EEDL2017

Figure 13. Collision stopping power (ionisation+excitation) calculated from the existing Livermore model and EEDL2017 for H, Fe and Pb. The relative difference is calculated according to equation (5). The energy scale is the same for both cross-sections and RD.

b) Excitation stopping power

As explained in section 3.3, the restricted ionisation stopping power is calculated according to equation (4). By setting T_{cut}=0.1 eV, the contribution to the energy loss induced by ionisation becomes 0. In this case, the stopping power obtained by ***ComputeDEDXPerVolume()*** method is the energy loss solely due to excitation. Figure 14 shows a part of the ***G4LivermoreIonisationModel::ComputeDEDXPerVolume()*** code. It is shown that the stopping power value this method returns is composed of ionisation and excitation stopping power. Moreover, ionisation stopping power is influenced by T_{cut} while excitation is not.

```
// loop for elements in the material
for (size_t iel=0; iel<NumberOfElements; iel++ )
  {
    G4int iZ = (G4int)((*theElementVector)[iel]->GetZ());
    G4int nShells = transitionManager->NumberOfShells(iZ);
    for (G4int n=0; n<nShells; n++)
  {
    G4double e = energySpectrum->AverageEnergy(iZ, minKineticEnergy: 0.0,cutEnergy,
                          kineticEnergy, n);
    G4double cs= crossSectionHandler->FindValue(iZ,kineticEnergy, n);
    sPower   += e * cs * theAtomicNumDensityVector[iel];
  }
    G4double esp = energySpectrum->Excitation(iZ,kineticEnergy);
    sPower   += esp * theAtomicNumDensityVector[iel];
  }

if (verboseLevel > 2)
  {
```

Stopping power due to ionisation, which depends on T_{cut} defined by cutEnergy)

Stopping power due to excitation, which is not influenced by T_{cut}

G4LivermoreIonisationModel::ComputeDEDXPerVolume

*Figure 14. Part of **G4LivermoreIonisationModel::ComputeDEDXPerVolume()** code.*

The comparison between the excitation stopping power obtained from EEDL2017 (EPICSHOW) and from the existing Livermore model, based on EEDL91 is shown in Figure 15. The results are remarkably close, which is expected, because the excitation cross-sections in EEDL2017 are very similar to EEDL91.

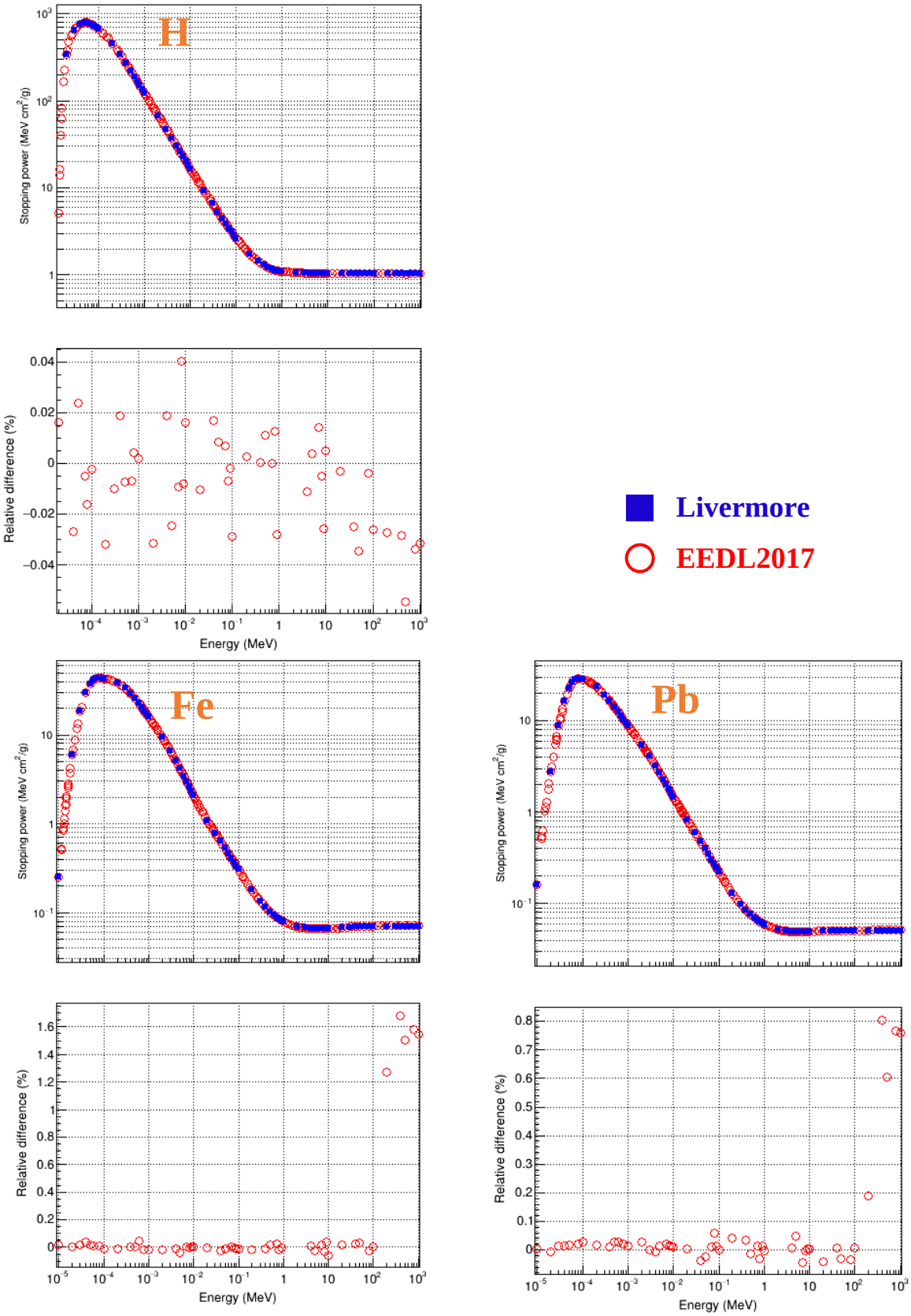

Figure 15. Excitation stopping power calculated from the existing Livermore model and EEDL2017 for H, Fe and Pb. The relative difference is calculated according to equation (5). The energy scale is the same for both cross-sections and RD.

c) Ionisation stopping power

As explained above, we have obtained by using the ***ComputeDEDXPerVolume()*** method:

- The collision stopping power $\mathrm{SP_{Collision}}$ with T_{cut} = 10 GeV (section 4.2.3 (a));
- The excitation stopping power $\mathrm{SP_{Excitation}}$, which is retrieved with T_{cut} = 0.1 eV in order to exclude the contribution of energy loss due to ionisation (section 4.2.3 (b)).

So, the stopping power solely due to ionisation is then calculated as follows:

$$\mathrm{SP_{Ionisation}} = \mathrm{SP_{Collision}} - \mathrm{SP_{Excitation}} \qquad (6)$$

The comparison between the ionisation stopping power obtained from EEDL2017 (EPICSHOW) and from the existing Livermore model, based on EEDL91 is shown in Figure 16. The results are very similar to the case of collision stopping power, with relative differences within a few percent. This is expected due to two reasons:

- The ionisation plays a dominant role in continuous energy loss.
- The difference of excitation stopping power between Livermore and EEDL2017 is negligible.

We can notice that for H, the relative difference is higher compared to other elements. Actually, a comparison between the stopping power values calculated from the parameterization in Livermore model and those directly obtained from EEDL91 tabulated data shows a similar difference for H (see section 4.2.4) Therefore, the higher relative difference observed in Figure 16 for H is only the consequence of the parameterization and not due to the update of EEDL2017. Thus, the parameterization for the calculation of stopping power, adopted in the Livermore ionisation model based on EEDL91, does not require a specific update for EEDL2017.

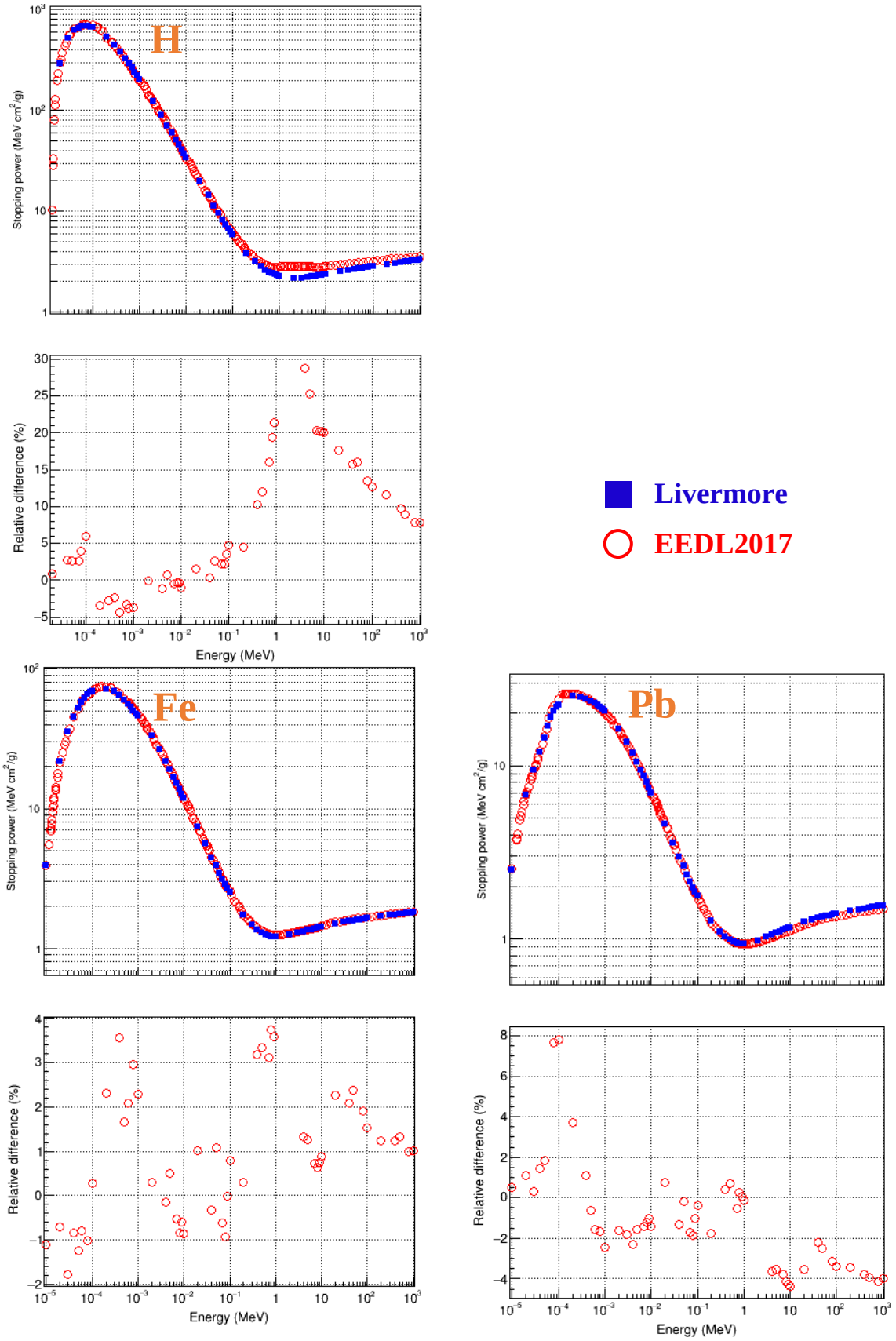

Figure 16. Ionisation stopping power calculated from the existing Livermore model and EEDL2017 for H, Fe and Pb. The relative difference is calculated according to equation (5). The energy scale is the same for both cross-sections and RD.

4.2.4. Comparison between EEDL91 and Livermore

Similar to section 4.2.2, we made approximate comparisons between Livermore and EEDL91 by superposing the Livermore graph on EEDL91 graph [10]. These rough comparisons are just for indicative purpose.

a) Collision stopping power

Figure 17 shows the comparison between EEDL91 and Livermore. The Livermore results were obtained with T_{cut} = 10 GeV, as shown in section 4.2.3 (a). We observe as expected that at low energies, Livermore is consistent with the total of EEDL9l. However, at high energies, we need to separate the contributions of excitation and ionisation to compare Livermore with EEDL91.

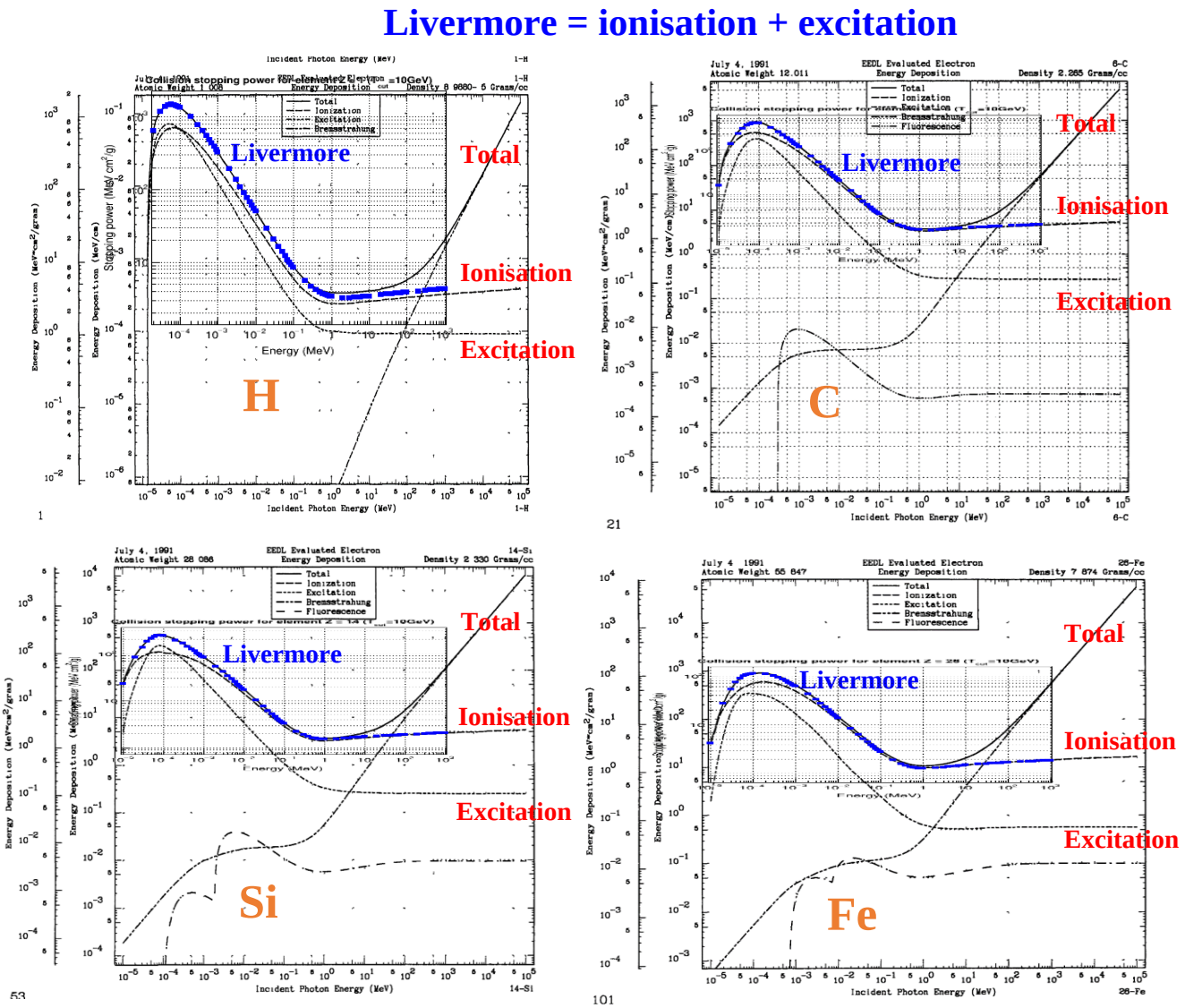

Livermore = ionisation + excitation

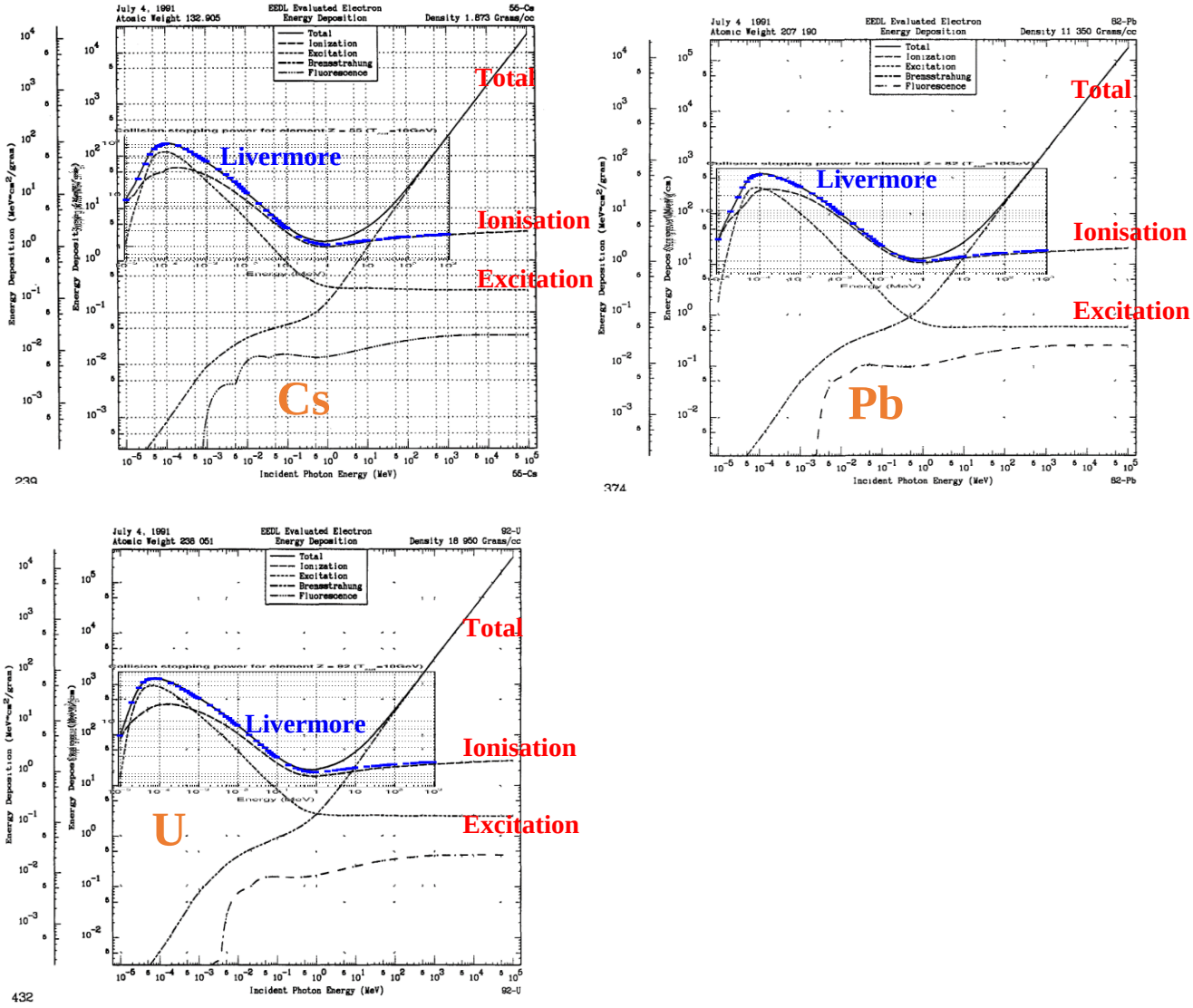

Figure 17. Comparison of stopping power (in unit MeV·cm^2/g) as a function of energy, for H, C, Si, Fe, Cs, Pb and U, between EEDL91 and the existing Livermore model when T_{cut} = 10 GeV.

b) Excitation stopping power

The comparisons of stopping power due to excitation are shown in Figure 18 for indicative purpose. We observe that Livermore model is in agreement with EEDL91 for excitation.

Livermore = excitation

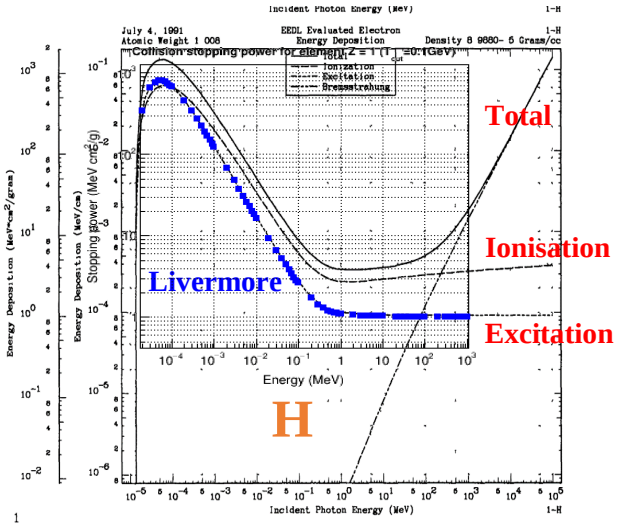

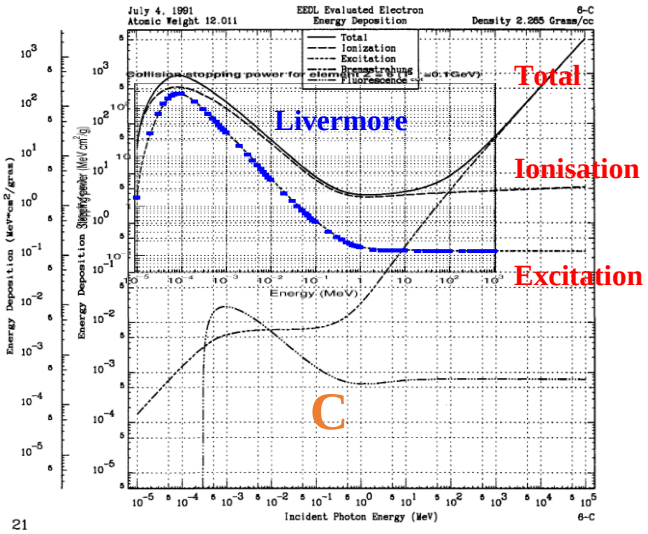

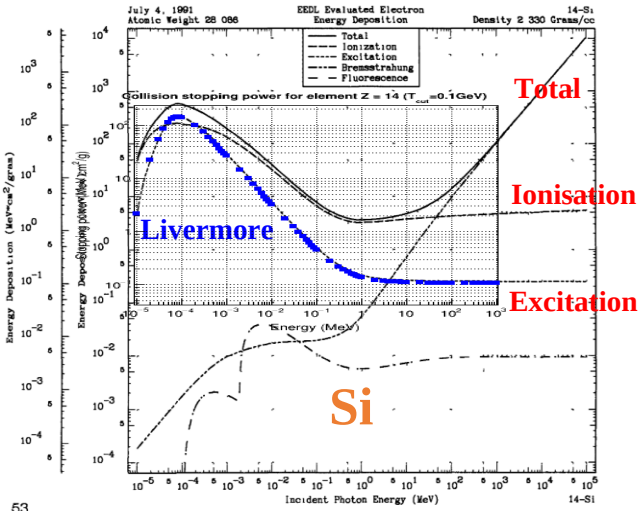

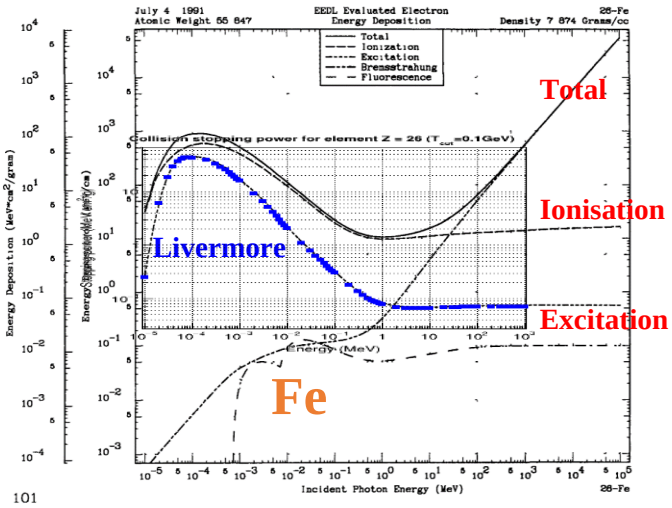

Livermore = excitation

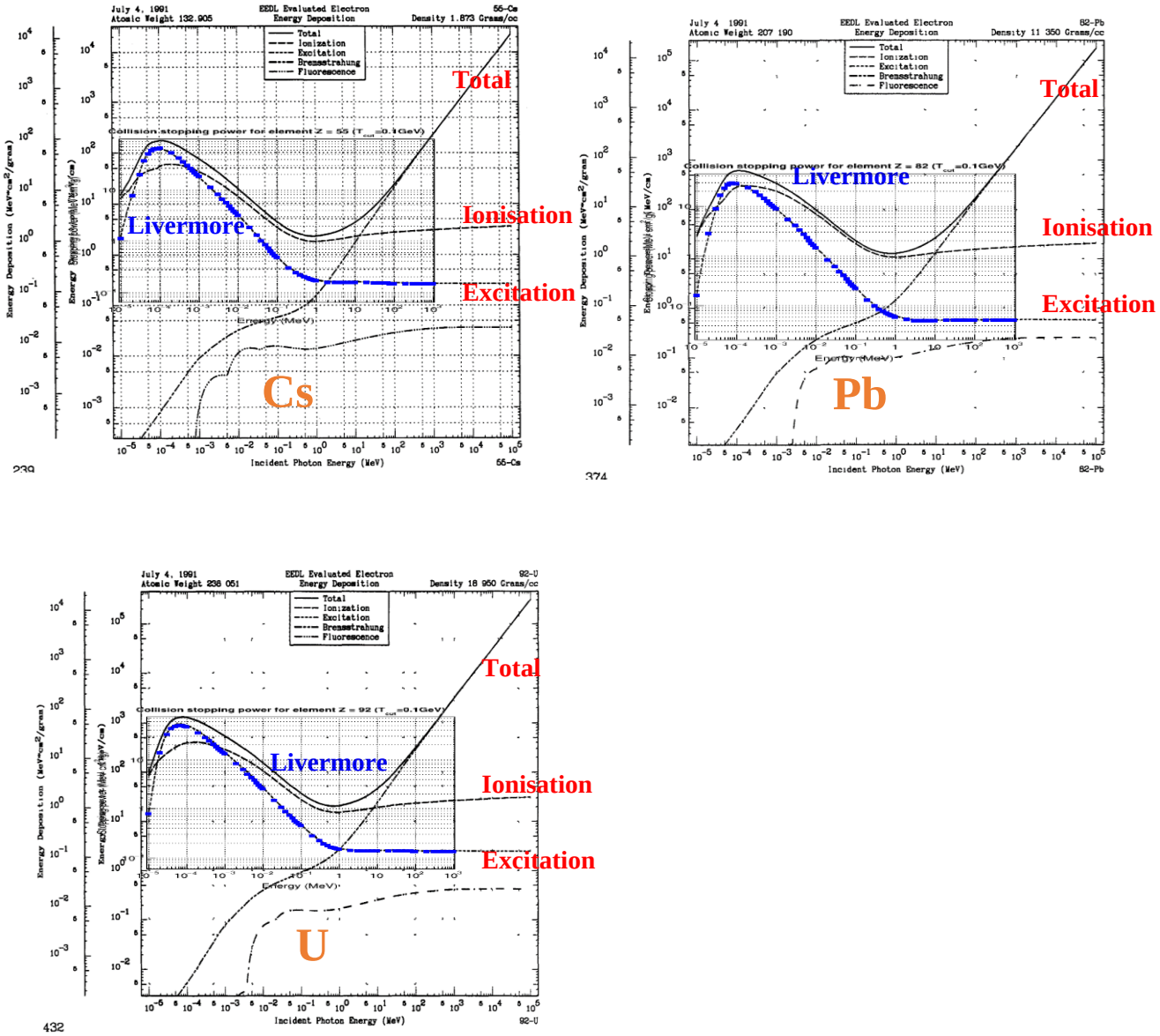

Figure 18. Comparison of stopping power (in unit MeV·cm^2/g) as a function of energy, due to excitation for H, C, Si, Fe, Cs, Pb and U, between EEDL91 and the existing Livermore model when T_{cut} = 0.1 eV.

c) Ionisation stopping power

Similarly, the comparisons of ionisation stopping power between Livermore and EEDL91 (Figure 19) are rough and just for indicative purpose. We observe a good agreement for the studied elements except a slight difference for H at ~1 MeV.

Livermore = ionisation

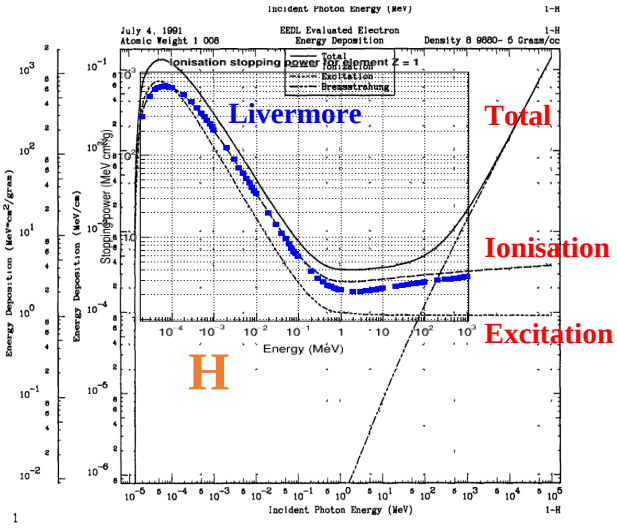

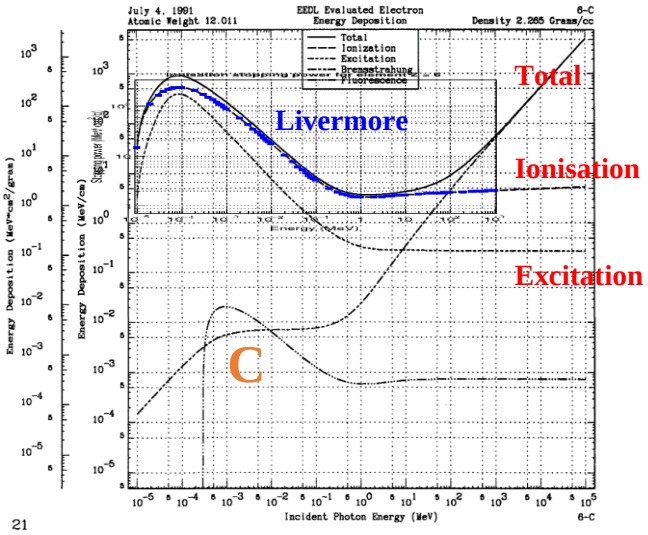

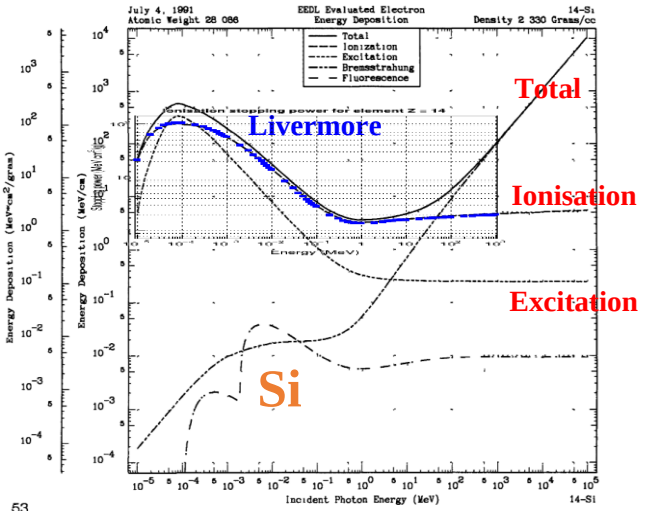

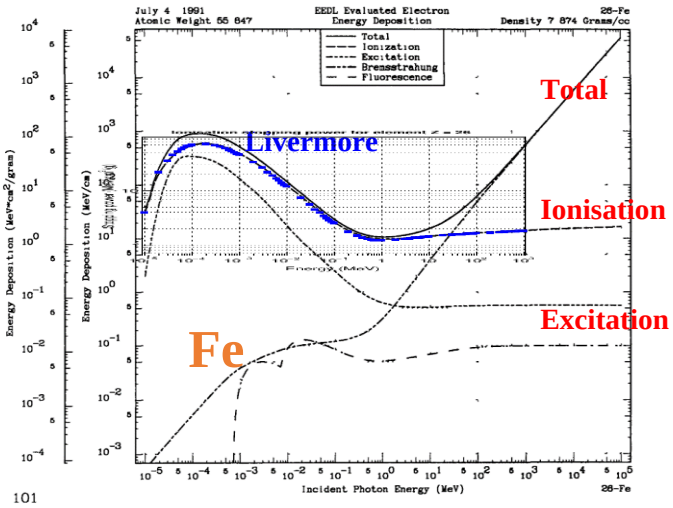

Livermore = ionisation

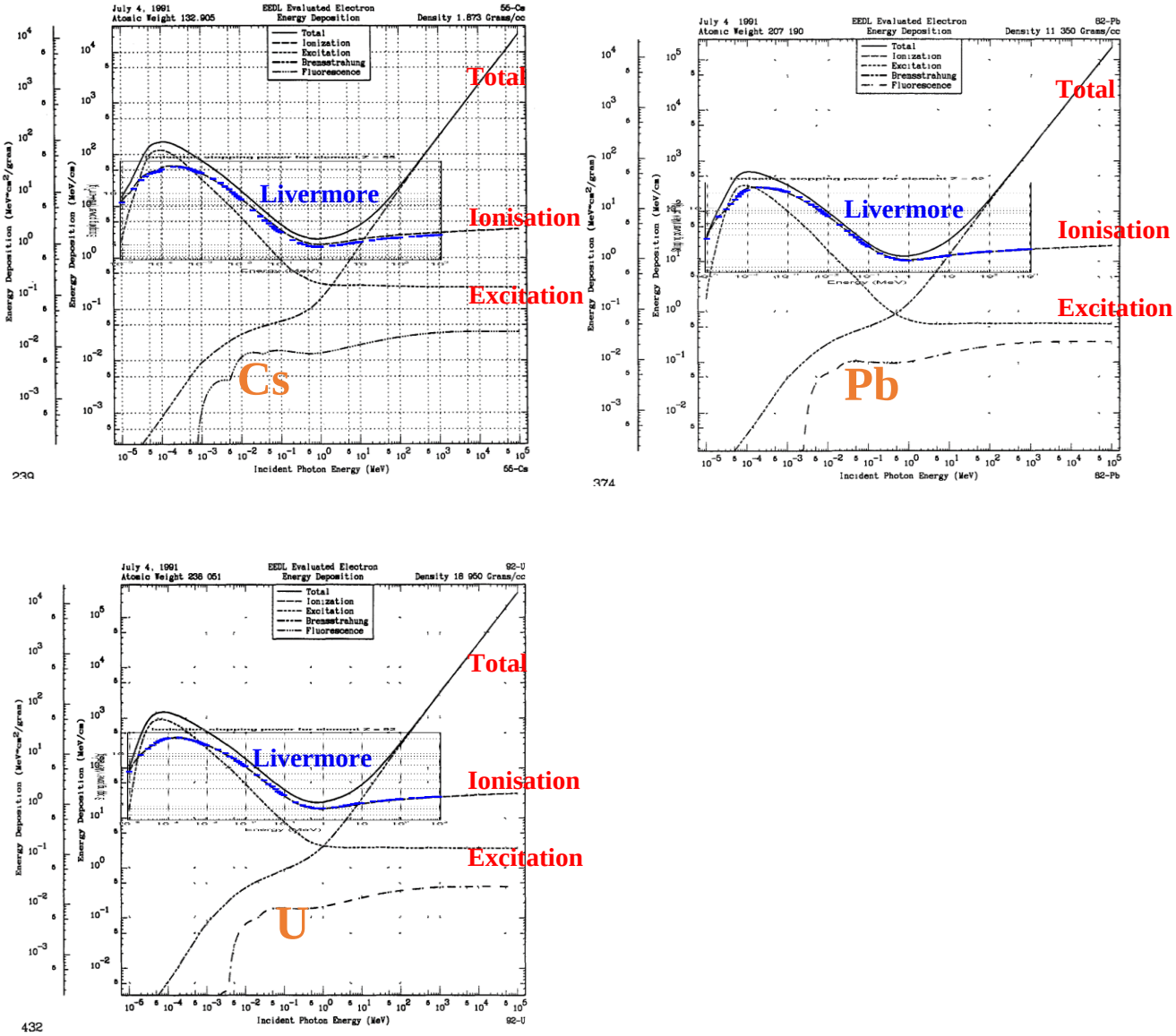

Figure 19. Comparison of stopping power (in unit MeV·cm^2/g) as a function of energy, due to ionisation for H, C, Si, Fe, Cs, Pb and U, between EEDL91 and the existing Livermore model.

5. Comparison of ionisation cross-section and stopping power among different models

In this section, we will compare the cross section and stopping power among different models:

- ***G4PenelopeIonisationModel***;
- ***G4MollerBhabhaModel***;
- ***G4LivermoreIonisationModel***.

5.1. Cross-section comparison for three models

To study the impact of T_{cut} on the cross-section, we plot the cross-section with different T_{cut}, as shown in Figure 20, calculated from the three models with T_{cut} = 10^{-5}, 0.01 and 0.1 eV. We observe that:

- For Livermore model: the cross-sections varies with T_{cut} when T_{cut} is below 0.1 eV, which is expected, since 0.1 eV is the low energy limit of secondary electron in EEDL as mentioned in section 3.2. This also implies the cross-section with T_{cut} below 0.1 is total ionisation cross section as explained in section 3.2.
- For Penelope model: the cross-sections does not vary with T_{cut} either. It was closer to Livermore than MollerBhabha. Besides, Penelope cross-section values are constant below 100 eV.
- For MollerBhabha model: the cross-section always varies with T_{cut}. The values with T_{cut} below 10 eV seems aberrant.

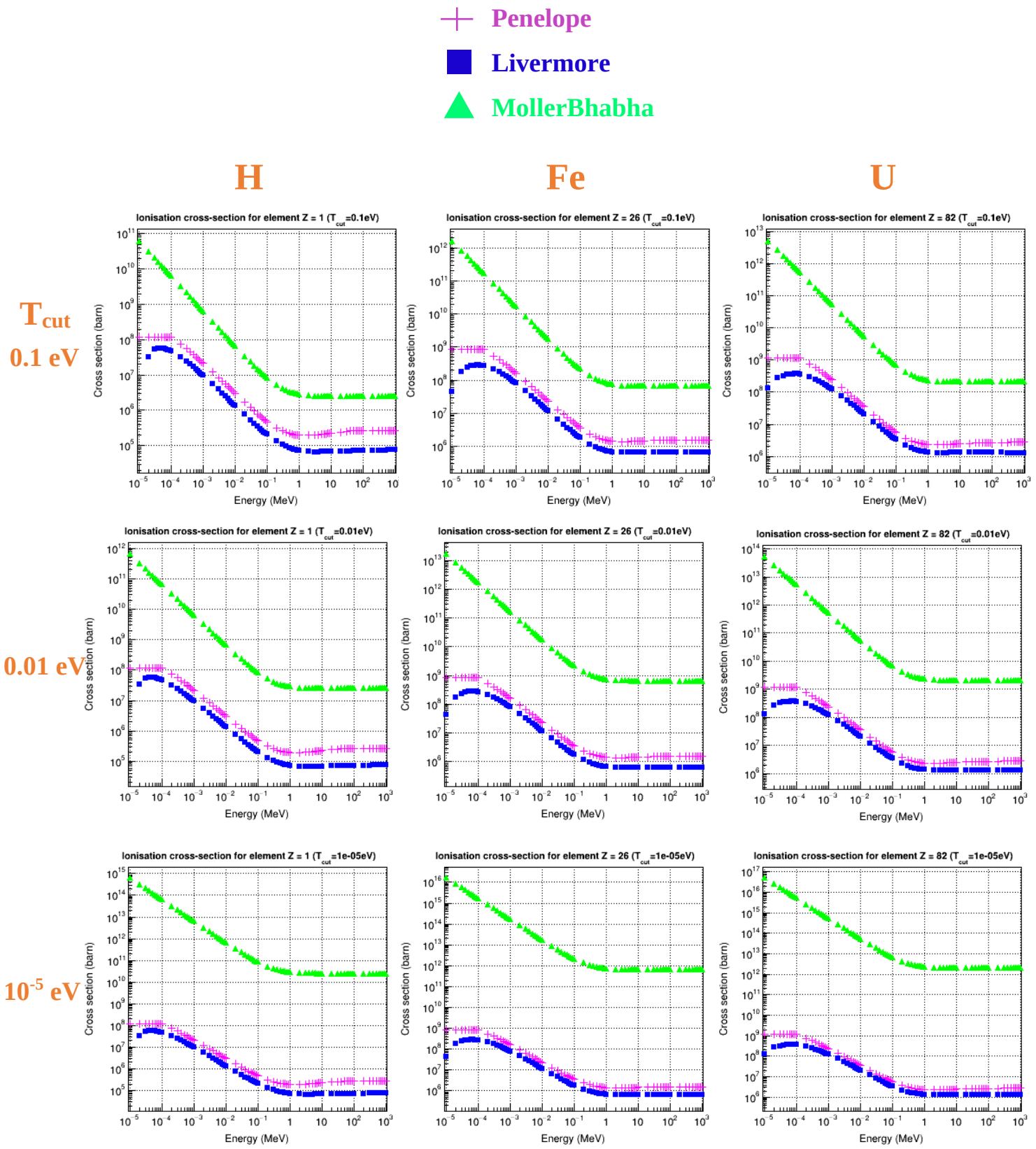

Figure 20. Ionisation cross-section as a function of energy for H, Fe and U, calculated from three models with T_{cut} = 0.1 eV, 0.01 eV and 10^{-5} eV.

Figure 20 shows the ionisation cross-section calculated from the three models with T_{cut} = 0.1 eV, 1 eV and 10 eV. We observed that:

- For Livermore model, the cross-sections are restricted cross-sections, varying with T_{cut}, which represents the cross-section of generation of an electron above T_{cut}.
- For Penelope model, the cross-sections keep identical when T_{cut} = 0.1 eV and 1 eV, and change when T_{cut}=10 eV.
- For MollerBhabha, the cross-sections gradually approach Livermore and Penelope as T_{cut} increases. The agreement with the other models seems to be better when T_{cut} was 10 eV.

Penelope

Livermore

MollerBhabha

	H	Fe	U
T_{cut} 10 eV	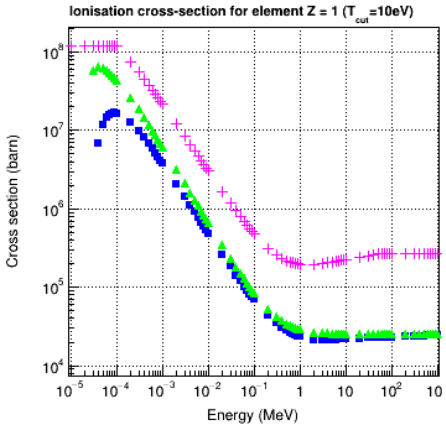	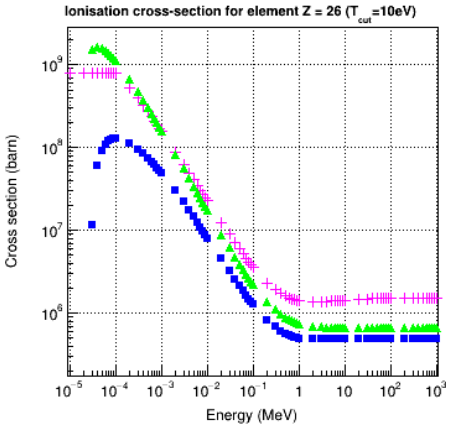	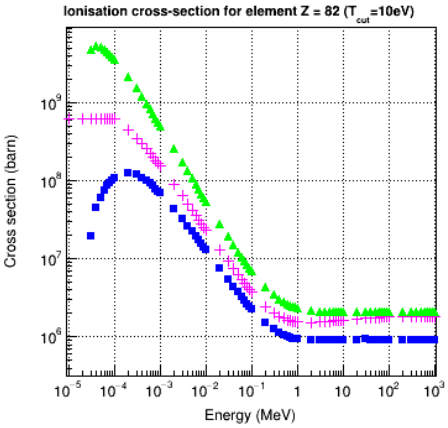
1 eV	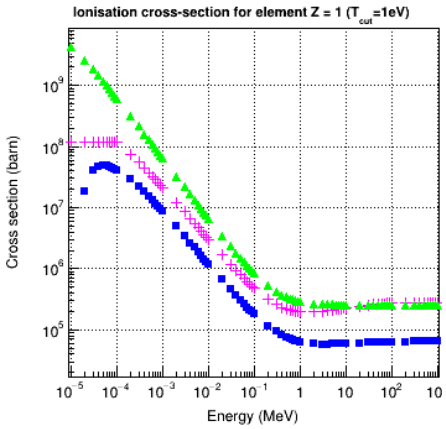	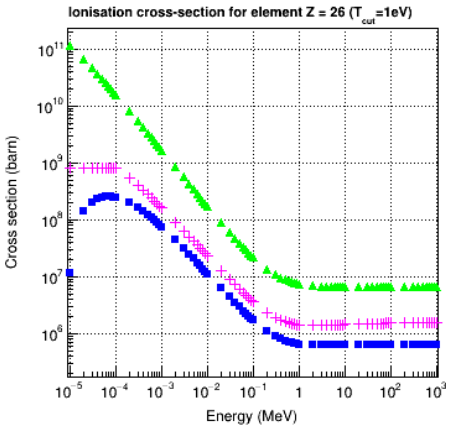	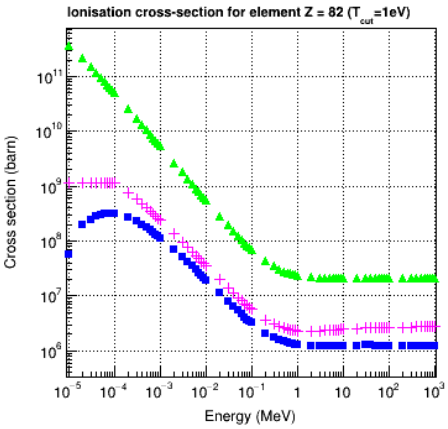
0.1 eV	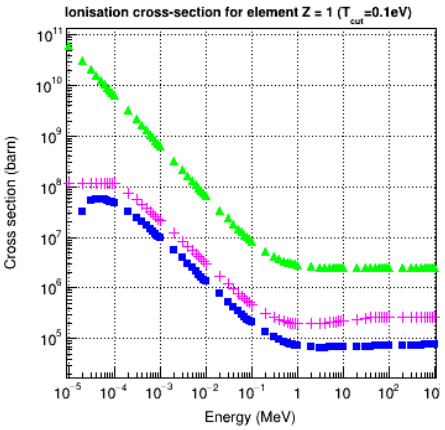	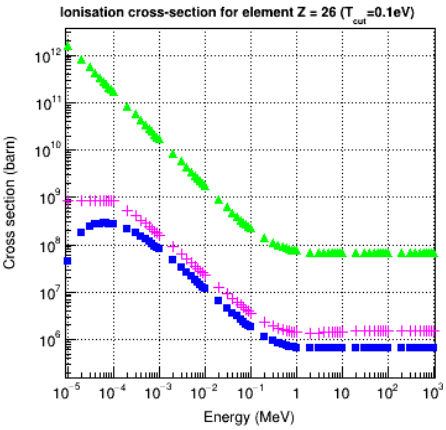	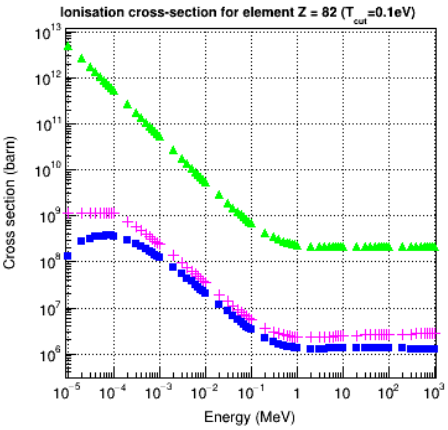

Figure 21. Ionisation cross-section as a function of energy for H, Fe and U, calculated from three models with T_{cut} = 10 eV, 1 eV, 0.1 eV.

5.2. Stopping power comparison for three models

Figure 22 shows the collision stopping power comparison calculated from three models. As already explained in section 4.2.3, to obtain the total collision stopping power, T_{cut} should be larger than the highest transferred energy. In our comparison, the energy of incident electron ranges from E=10 eV-1 GeV. So in this case, $T_{max} = 0.5E = 0.5$ GeV. So any T_{cut} above 0.5 GeV will not change the results of total collision stopping power. Here we took T_{cut}=10 GeV. The three models are in agreement, the main differences are observed at low energies. As already observed for cross-section, stopping power calculated by Penelope model is constant below 100 eV.

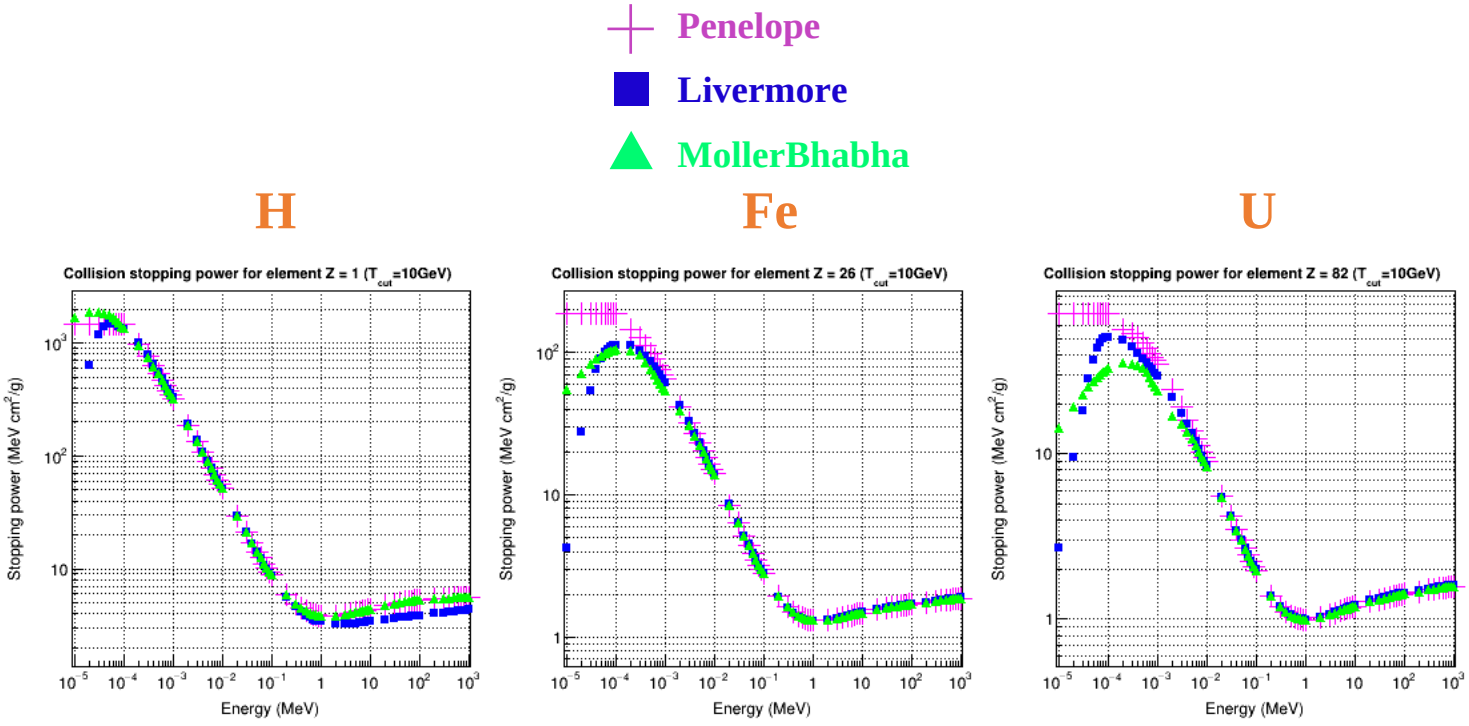

Figure 22. Collision stopping power comparison of H, Fe and U, calculated from three models with T_{cut} = 10 GeV.

6. Comparison of stopping power with other data sources

In this section, the data sources that we used are as follows:

- ESTAR (Stopping Powers and Ranges for Electrons) [11] is a NIST database [1], which provides separately collision and radiative stopping power for electrons in various materials, over the energy range **10^{-3} - 10^{4} MeV**.
- ICRU90 [12], provides separately collision and radiative stopping power for air, graphite and water materials;
- Three Geant4 models (Penelope, Livermore and MollerBhabha):
    - For elements Z=1-97;
    - For materials: G4_AIR, G4_GRAPHITE, G4_WATER, and user-defined H_2O with different mean excitation energy values.

6.1. EPICS2017 VS ESTAR

Figure 23 shows the collision stopping power for H, C, Si, Fe, Cs, Pb, U between EPDL2017 and ESTAR. In general, EPDL2017 is in agreement with ESTAR over the energy range 10^{-2} - 10^{4} MeV. At lower energies, we can observe a disagreement between the two databases:

- For C, Si, Fe, Cs, Pb, U:
    - In the range of 10^{-2} - 10^{3} MeV, the relative difference (RD) is less than 6%.
    - In the range of 10^{-3} - 10^{-2} MeV, RD is much bigger, and it becomes bigger and bigger as the energy decreases, especially for heavy elements.
- For H, in the range of 10^{-3} - ~3 MeV, RD is less than 5%. In the range of ~3 – 10^{3} MeV, RD is up to 20%, it becomes bigger and bigger as the energy increases.

[1] The NIST data is available via https://physics.nist.gov/PhysRefData/Star/Text/ESTAR.html.

ESTAR

EEDL2017

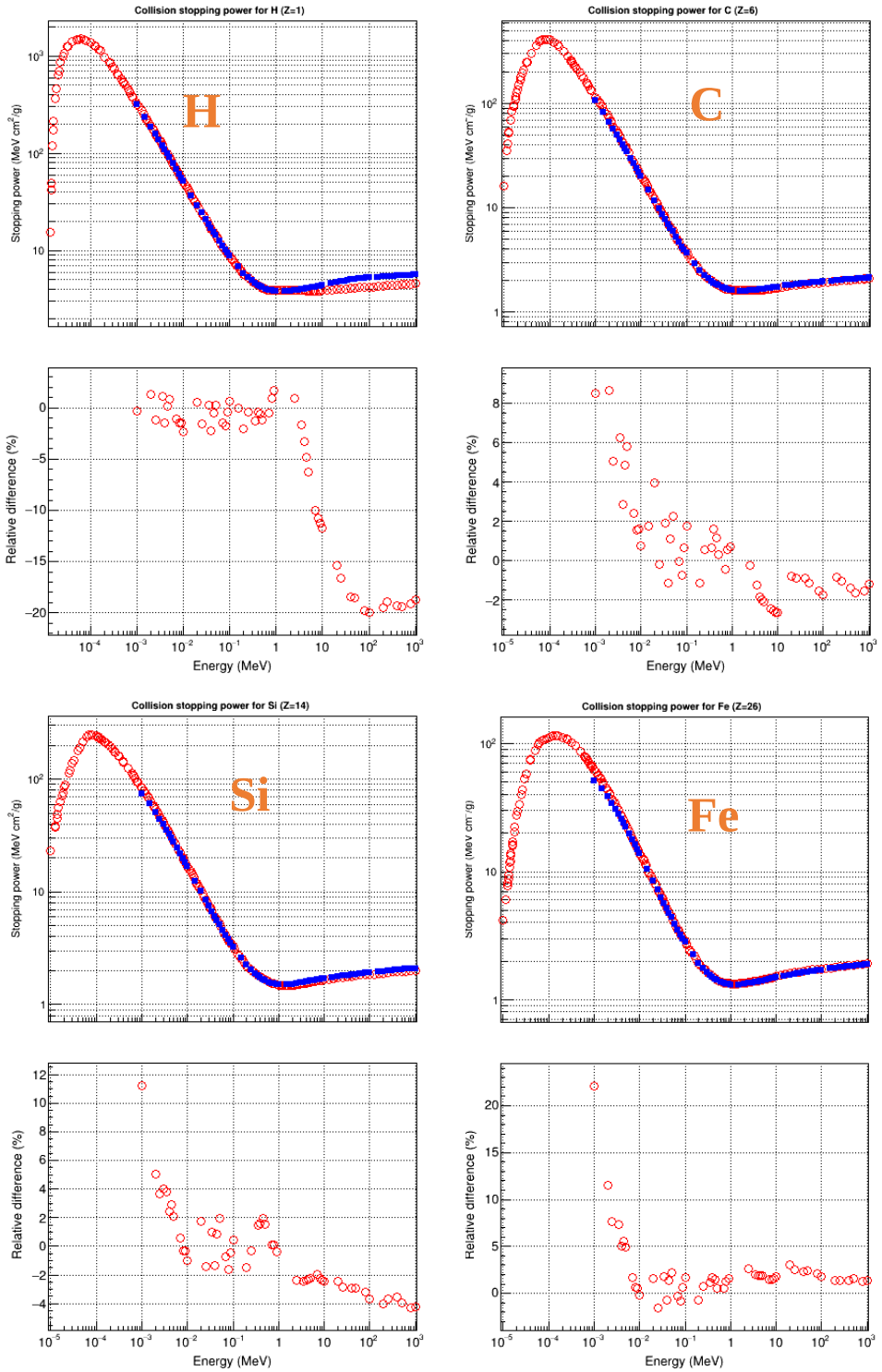

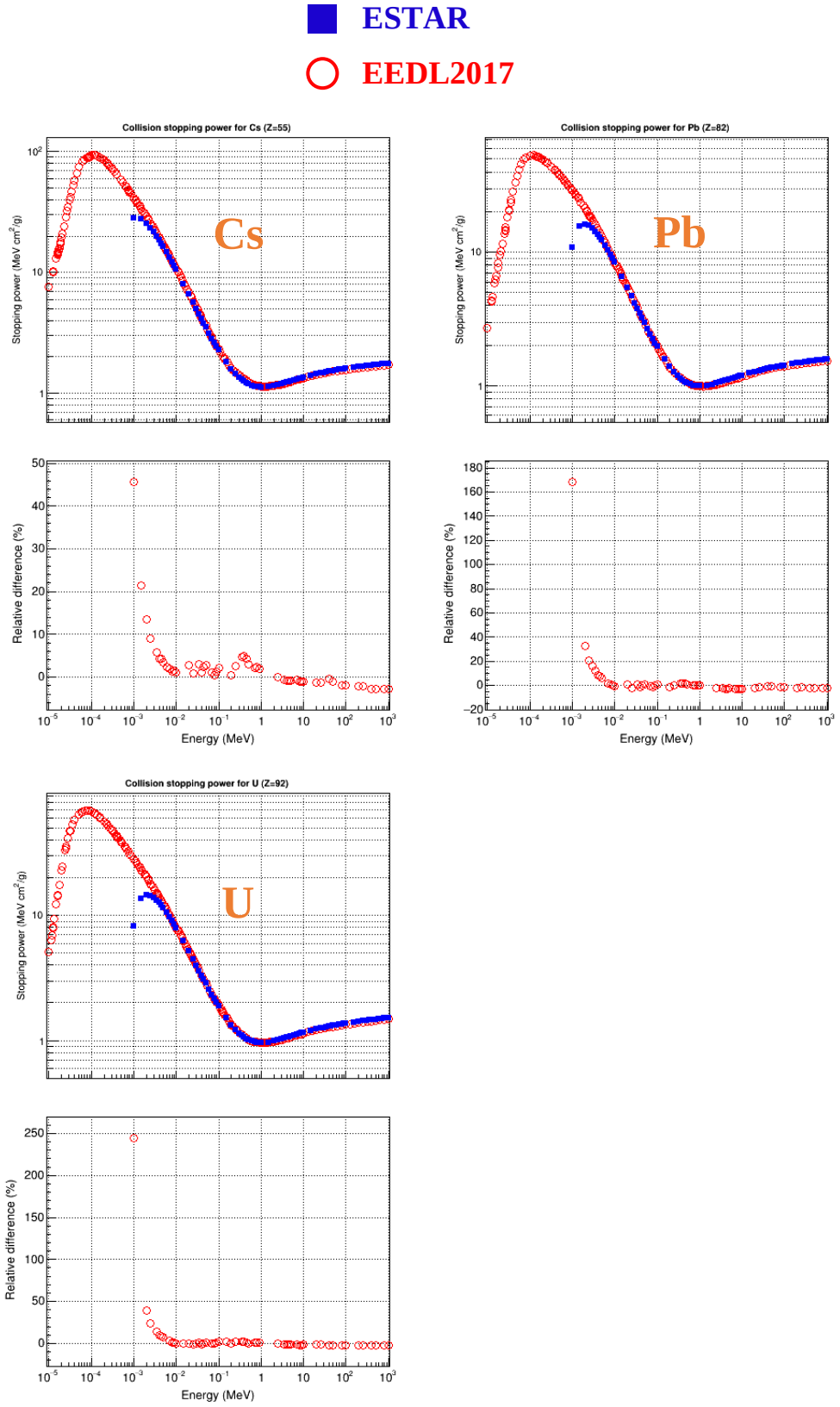

Figure 23. Comparison of stopping power for H, C, Si, Fe, Cs, Pb, U between EPDL2017 and ESTAR.

6.2. ICRU90 VS ESTAR

Figure 24 shows the stopping power between ICRU90 and ESTAR for air, graphite and water:

- For air, ICRU90 is the same as ESTAR.
- For graphite and water, the relative difference is less than 1.6%.

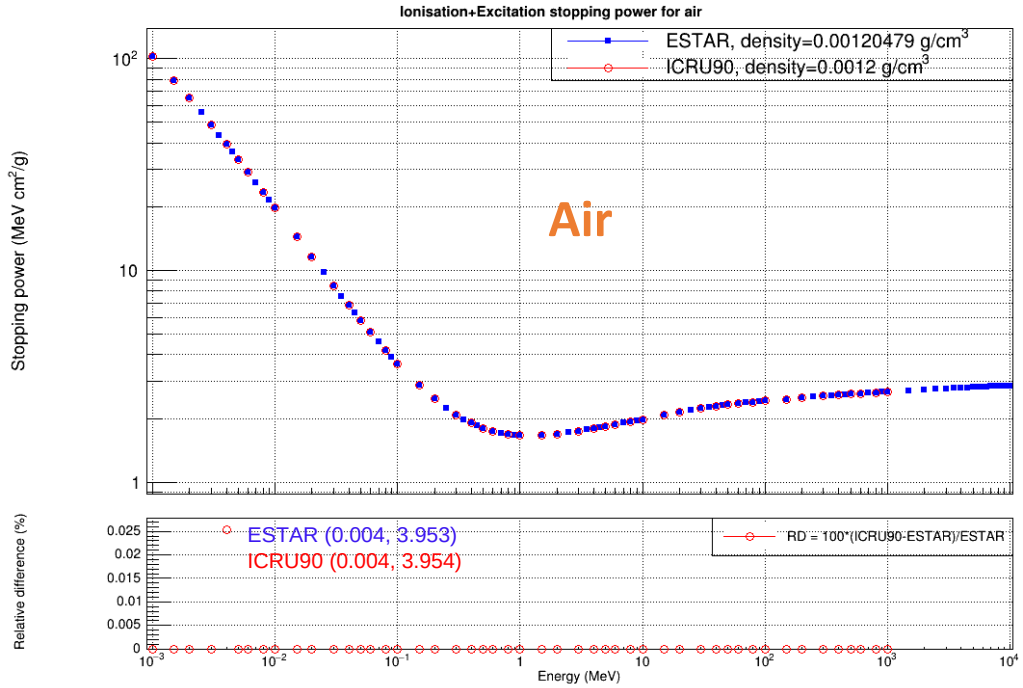

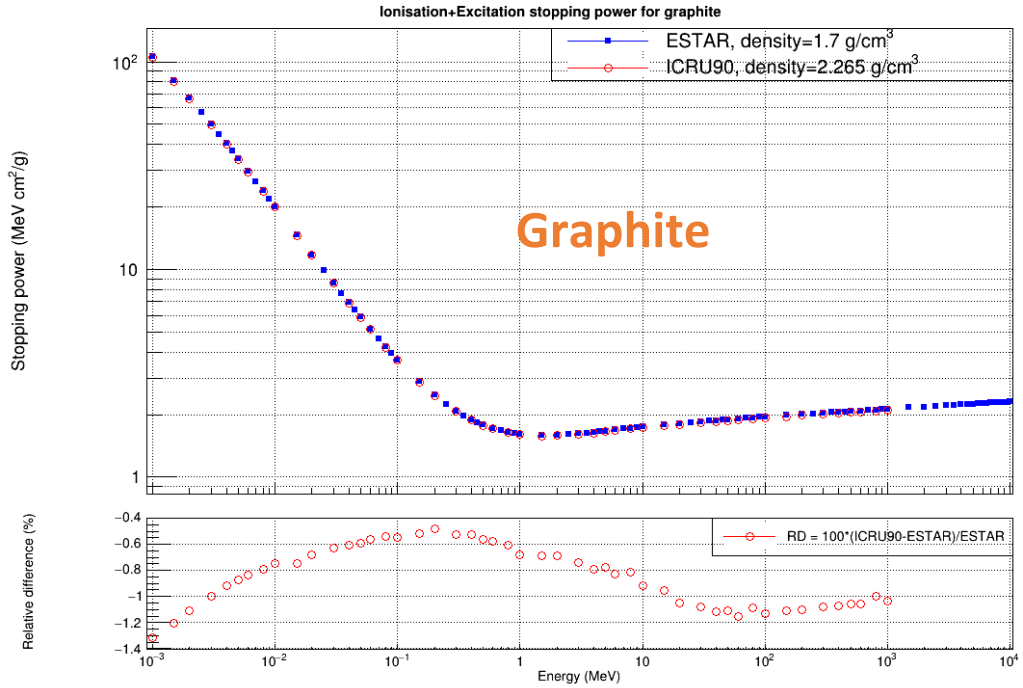

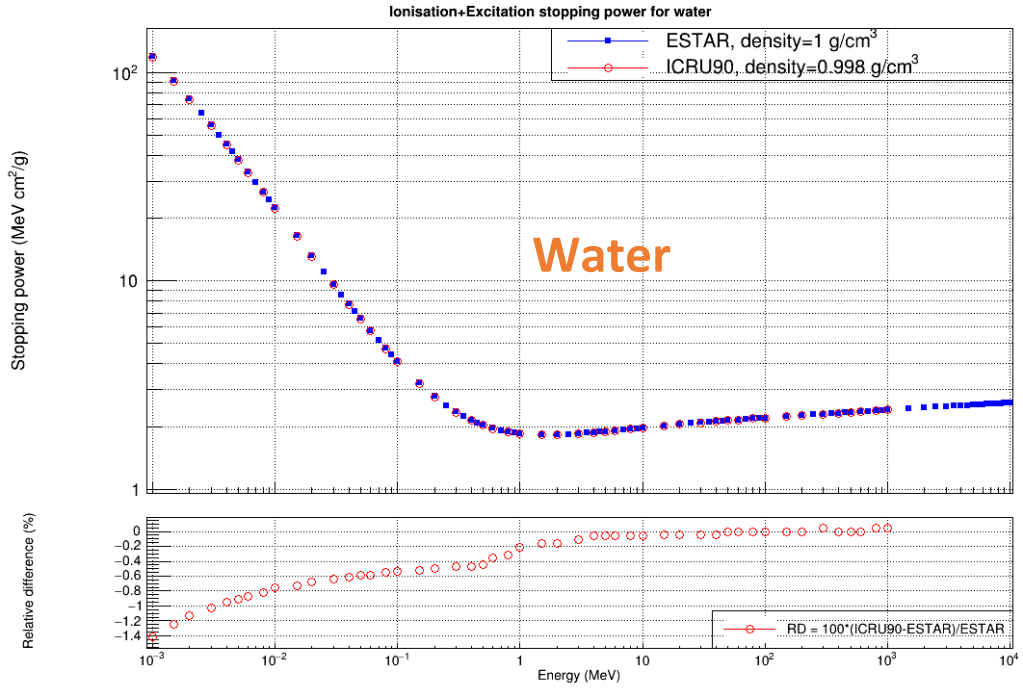

Figure 24. Comparison of stopping power for air, graphite and water between ICRU90 and ESTAR.

6.3. Three models VS ESTAR

Since the high energy limit for ESTAR is 10^4 MeV, we expanded the energy range during the simulation for three models. The energy range is 10^{-5} - 10^4 MeV. So in this case, to obtain the total collision stopping power, we should take T_{cut} larger than 10^4 MeV/2 = 5 GeV. We took T_{cut} = 20 GeV.

6.3.1. Elements

Figure 25 shows the stopping power of three models and ESTAR for elements H, C, Si, Fe, Cs, Pb, U. ***The relative difference of three models is calculated with respect to ESTAR***.

- For Penelope and MollerBhabha:
  - In the range of 10^{-2} - 10^4 MeV, a good agreement is observed between the two models and ESTAR. RD is less than 8%.
  - In the range of 10^{-3} - 10^{-2} MeV, difference from ESTAR becomes bigger, especially for heavy elements.
- For Livermore:
  - In the range of 10^{-2} - 10^4 MeV, generally there is a good agreement (RD is less than 6%) except for Z = 1, 2, 7-10, 17, 18, 35, 36, 54, 86, for which RD is relatively larger, up to 30% (for H).
  - In the range of 10^{-3} - 10^{-2} MeV, RD is worse. **Note that we did not put all figures in this technical note, but they can be found in the supplementary data.**

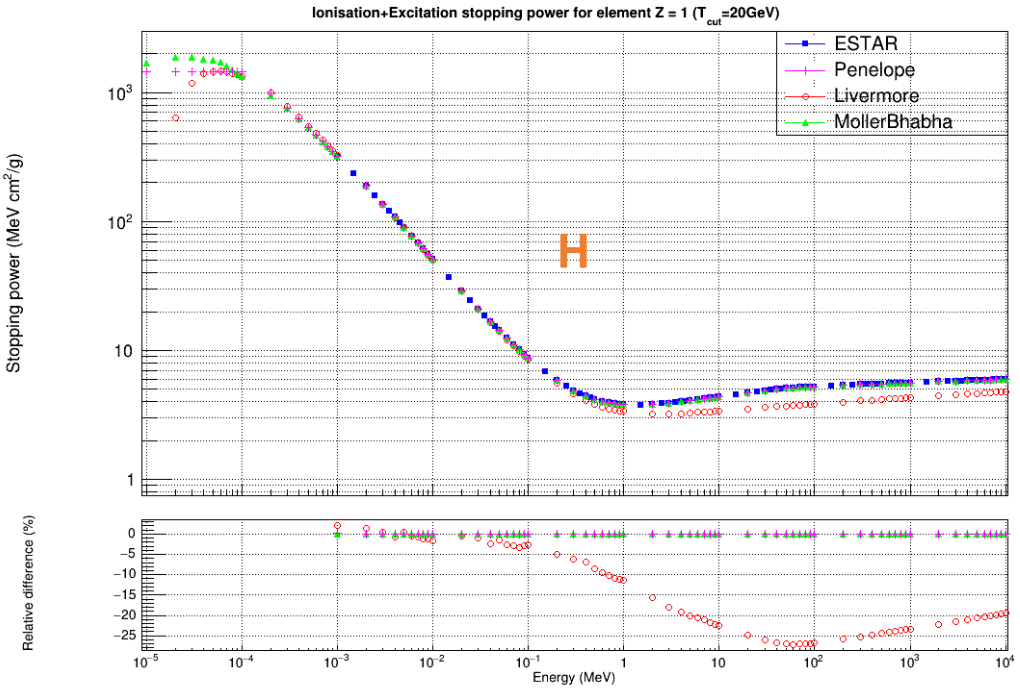
Ionisation+Excitation stopping power for element Z = 1 (T_cut=20GeV)
ESTAR
Penelope
Livermore
MollerBhabha
H
Stopping power (MeV cm²/g)
Relative difference (%)
Energy (MeV)

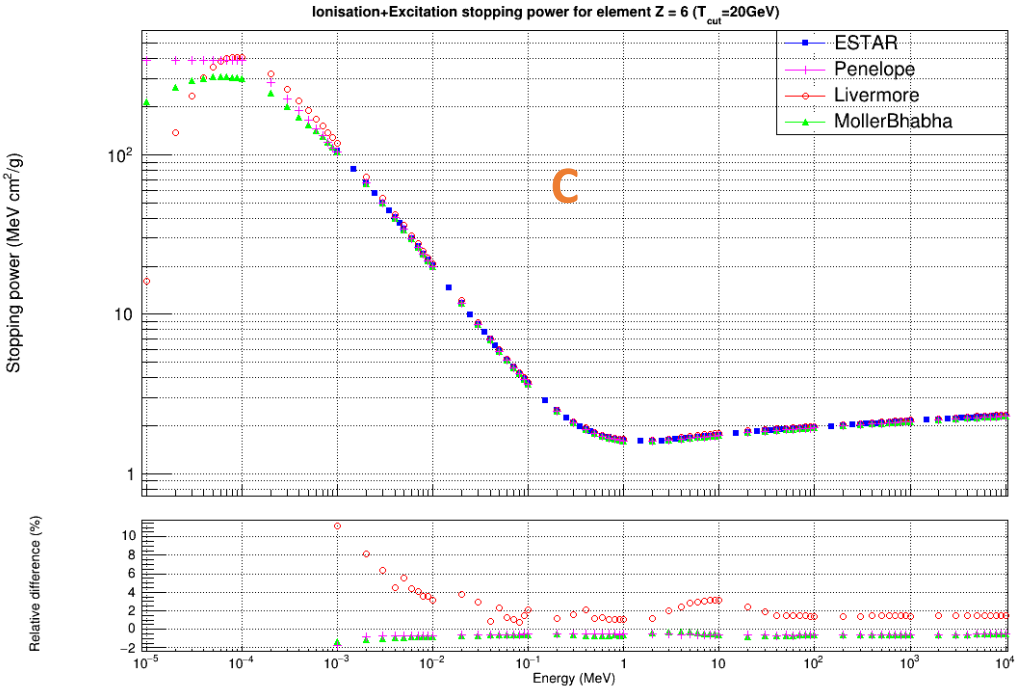
Ionisation+Excitation stopping power for element Z = 6 (T_cut=20GeV)
ESTAR
Penelope
Livermore
MollerBhabha
C
Stopping power (MeV cm²/g)
Relative difference (%)
Energy (MeV)

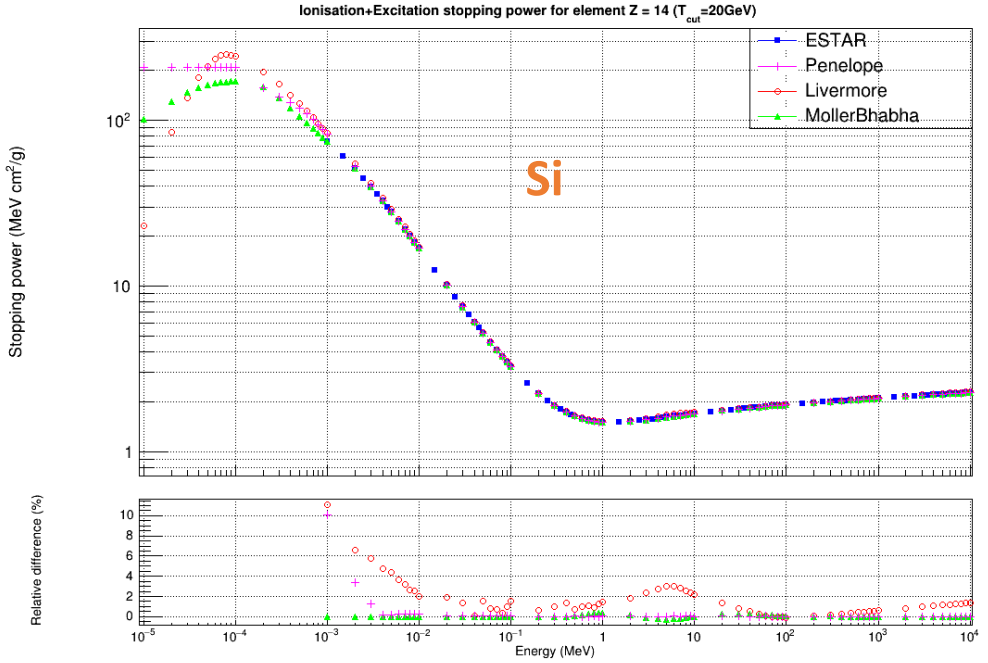
Ionisation+Excitation stopping power for element Z = 14 (T_cut=20GeV)
ESTAR
Penelope
Livermore
MollerBhabha
Si
Stopping power (MeV cm²/g)
Relative difference (%)
Energy (MeV)

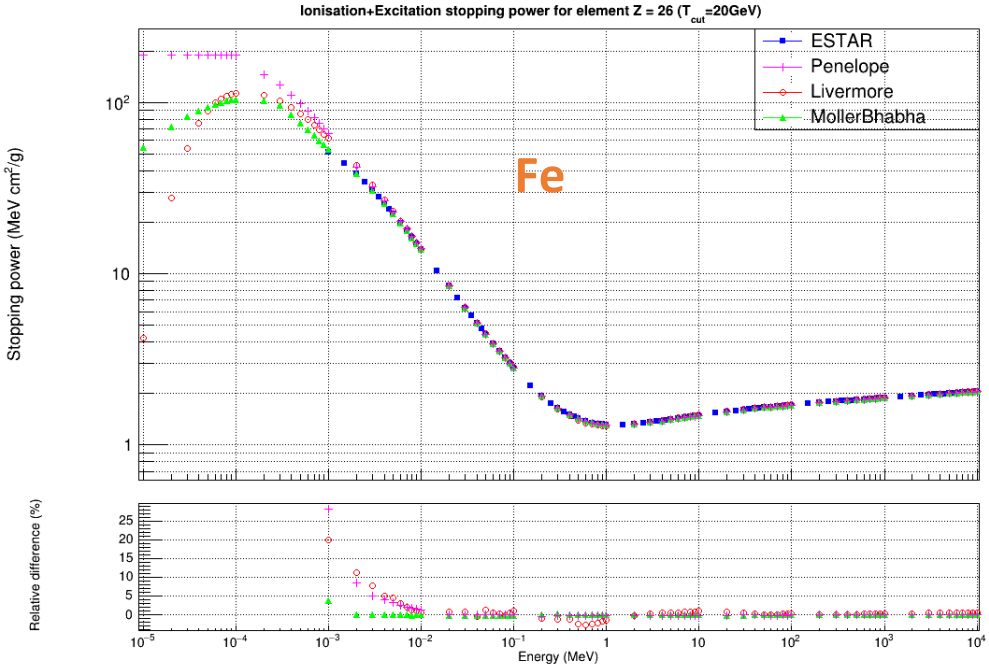
Ionisation+Excitation stopping power for element Z = 26 (T_cut=20GeV)
ESTAR
Penelope
Livermore
MollerBhabha
Fe
Stopping power (MeV cm²/g)
Relative difference (%)
Energy (MeV)

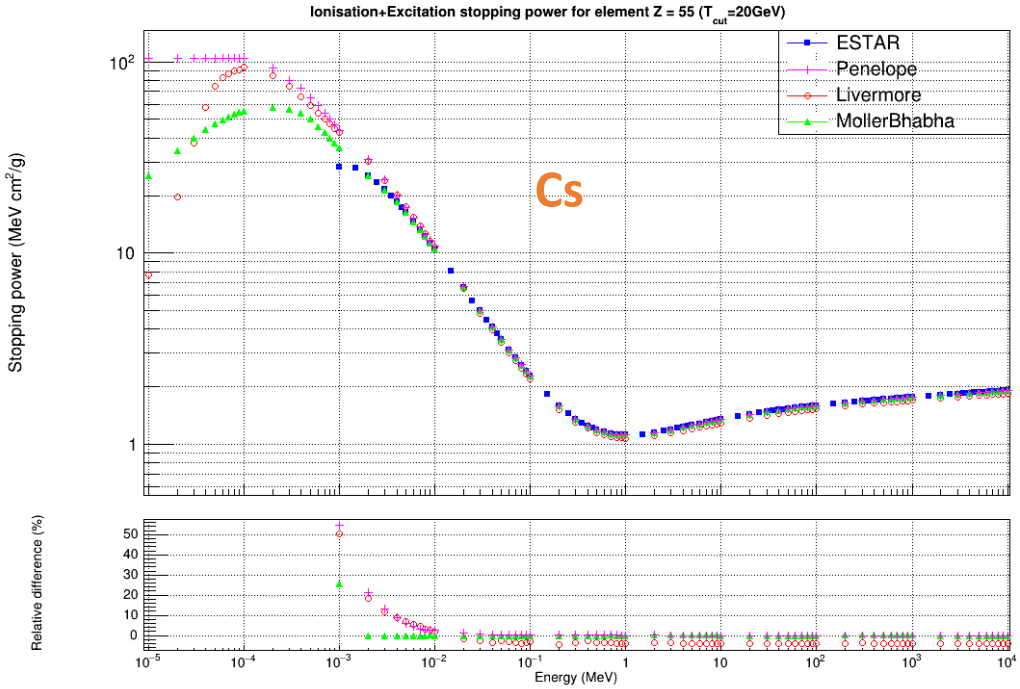
Ionisation+Excitation stopping power for element Z = 55 (T_cut=20GeV)
ESTAR
Penelope
Livermore
MollerBhabha
Cs
Stopping power (MeV cm²/g)
Relative difference (%)
Energy (MeV)

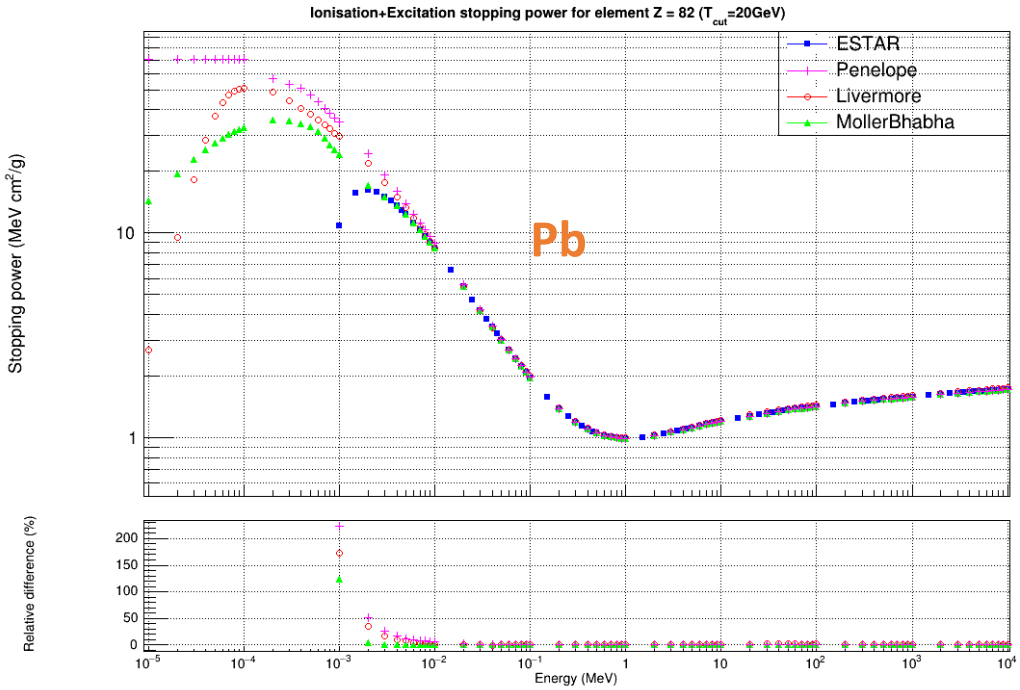
Ionisation+Excitation stopping power for element Z = 82 (T_cut=20GeV)
ESTAR
Penelope
Livermore
MollerBhabha
Pb
Stopping power (MeV cm²/g)
Relative difference (%)
Energy (MeV)

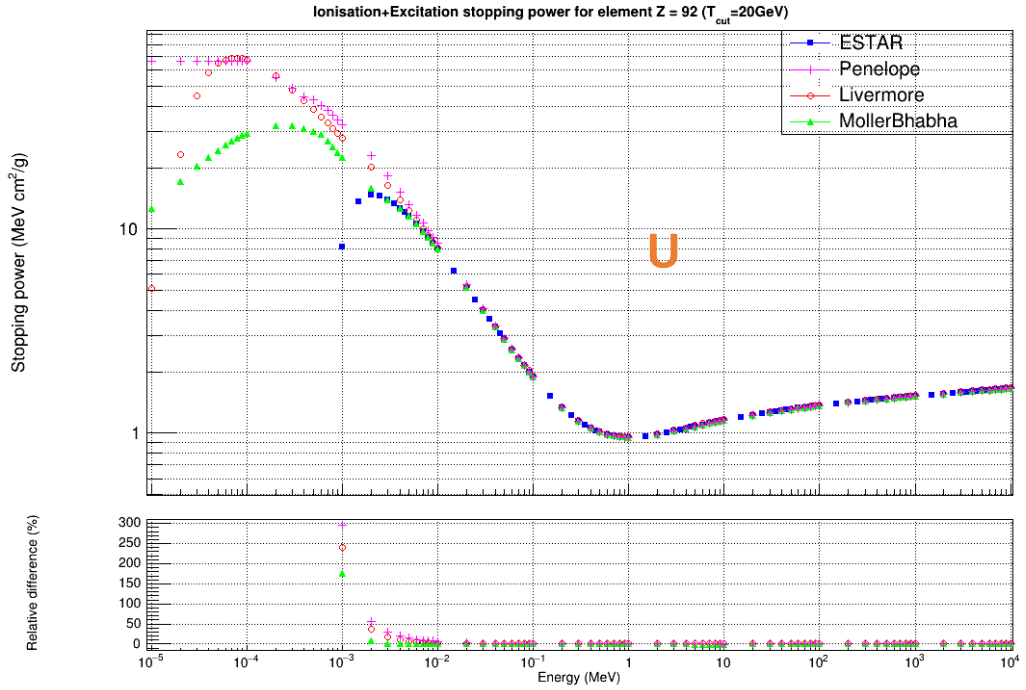

Figure 25. Comparison of stopping power between three models and ESTAR for elements.

In general, Penelope and MollerBhabha show a better agreement with ESTAR than Livermore. Moreover, a study on electron backscattering simulation[2], performed by Mihaly Novak, showed that using the PENELOPE ionisation model gives better agreement with the experimental data (Figure 26). For these reasons, from Geant4 11.2, **G4EmLivermorePhysics** and ***G4EmStandardPhysics_option4***, ionisation process is modelled by:

- ***G4PenelopeIonisationModel*** below 100 keV,
- ***G4MollerBhabhaModel*** above 100 keV

In the past (Geant4 11.1 and before), **G4EmLivermorePhysics** and ***G4EmStandardPhysics_option4*** used ***G4LivermoreIonisationModel*** below 100 keV.

[2] This was presented at the 27th Geant4 Collaboration Meeting, 26-30 September 2022, by Vladimir Ivantchenko "Status of EM physics". This presentation is available via: https://indico.cern.ch/event/1156193/contributions/5053237/attachments/2516417/4361500/StatusEM.pdf.

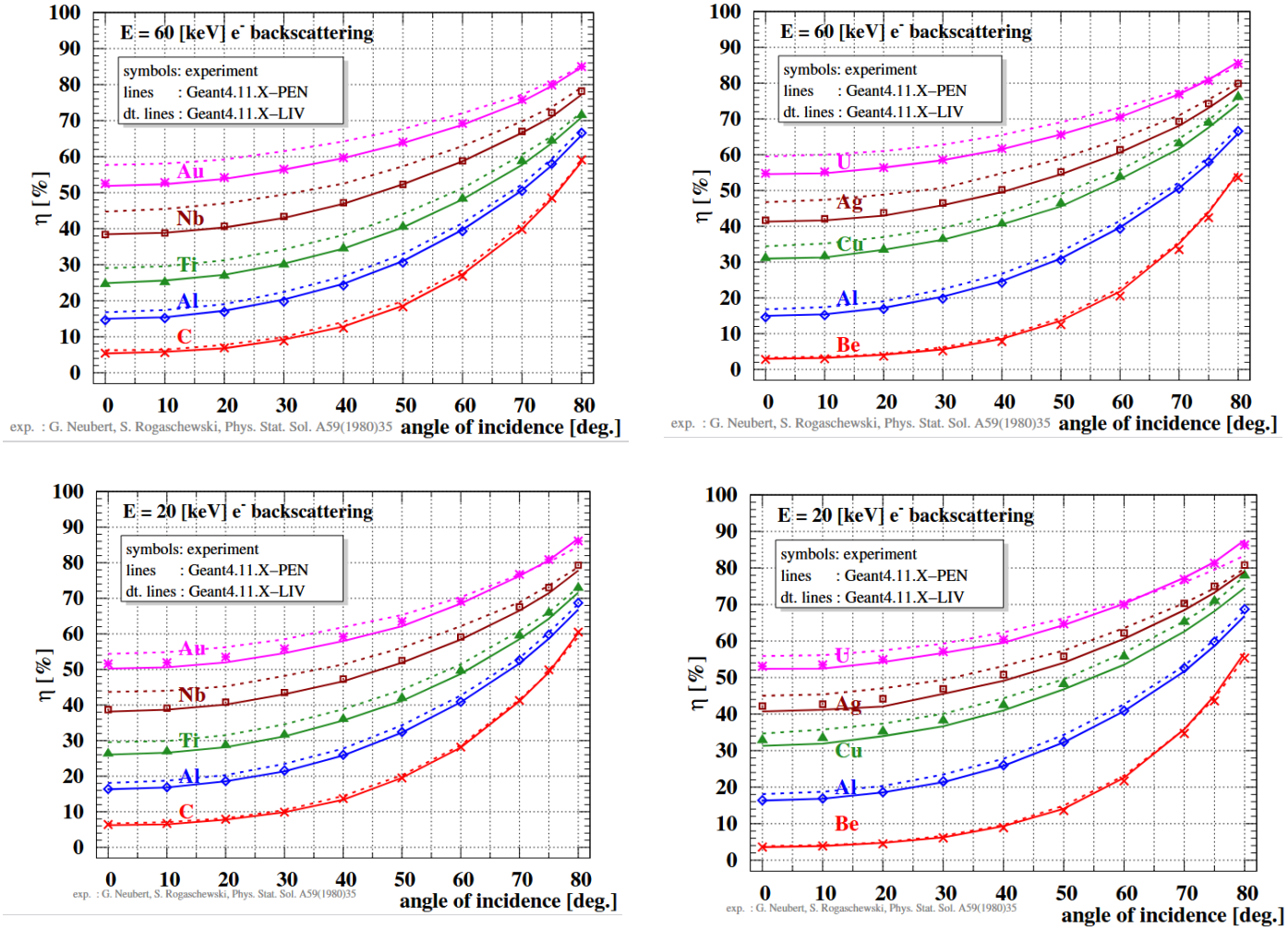

Figure 26. Low energy (20 and 60 keV) electron backscattering coefficient as a function of the incoming angle (measured from the surface normal) using the Penelope (PEN) and Livermore (LIV) EM constructors.

6.3.2. Air and graphite

Figure 27 shows the stopping power for air and graphite:

- Penelope and MollerBhaha are much closer (RD is less than 2%) to ESTAR than Livermore, especially at high energies.
- Livermore: RD is up to 18% for air, it becomes bigger and bigger above 1 MeV as the energy increases. RD is up to 12% for graphite.

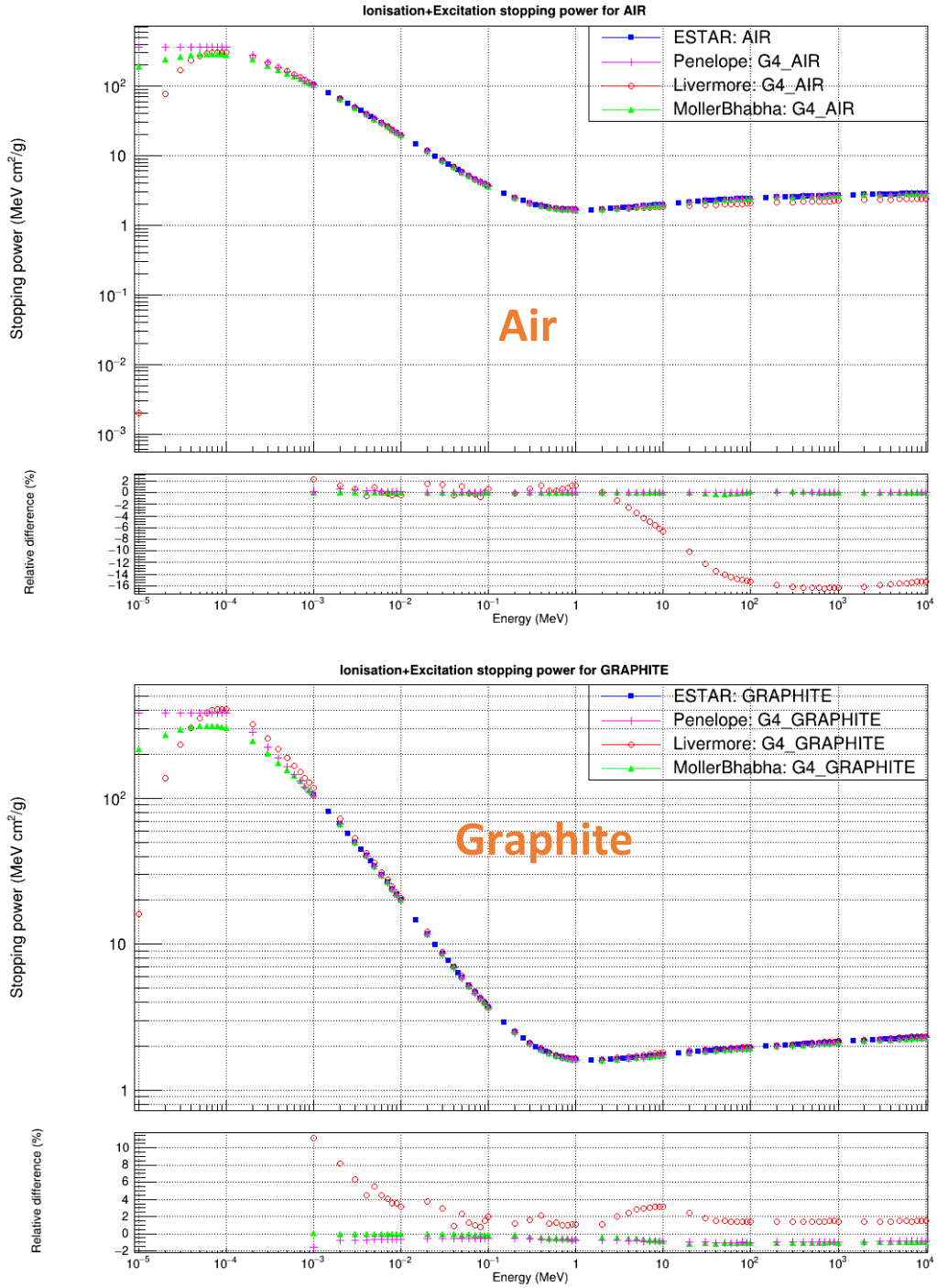

Figure 27. Comparison of stopping power between three models and ESTAR for air and graphite.

6.3.3. Water

As the mean excitation energy of a material plays a central role in the collision stopping power for electrons [12], we carried out comparison simulation for water with different mean excitation energy. The mean excitation energy for ESTAR water and G4_WATER are 75 eV and 78 eV respectively. In order to check the impact of the mean excitation energy value, we also build a user-defined H_2O with

75 and 78 eV of mean excitation energy. Figure 28 shows the stopping power of these four materials for each model separately. ***The relative difference is calculated with respect to ESTAR***:

- For Livermore and Penelope, there is no difference between defined H_2O with 75 eV or 78 eV. G4_WATER is very close to H_2O with 75 eV/78 eV.
- For MollerBhabha:
    - At low energies below 1 MeV, H_2O with 75 eV is much closer to ESTAR, which is expected as the mean excitation energy for ESTAR is also 75 eV.
    - Above 1 MeV, G4_WATER (78 eV) is closer to ESTAR (75eV).

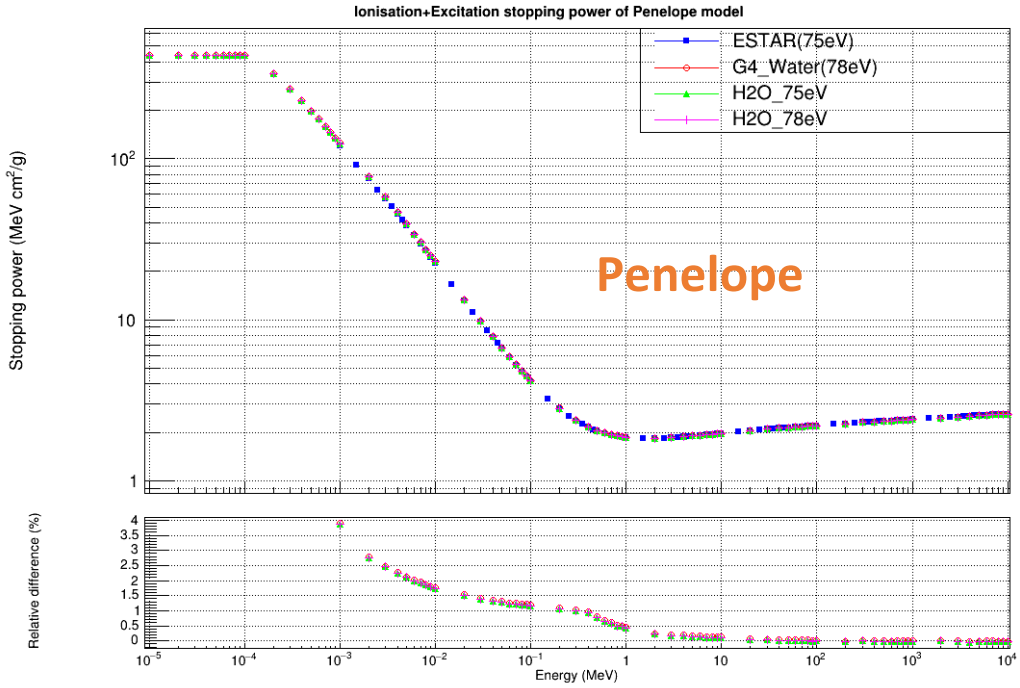
Ionisation+Excitation stopping power of Penelope model
ESTAR(75eV)
G4_Water(78eV)
H2O_75eV
H2O_78eV
Penelope
Stopping power (MeV cm²/g)
Relative difference (%)
Energy (MeV)

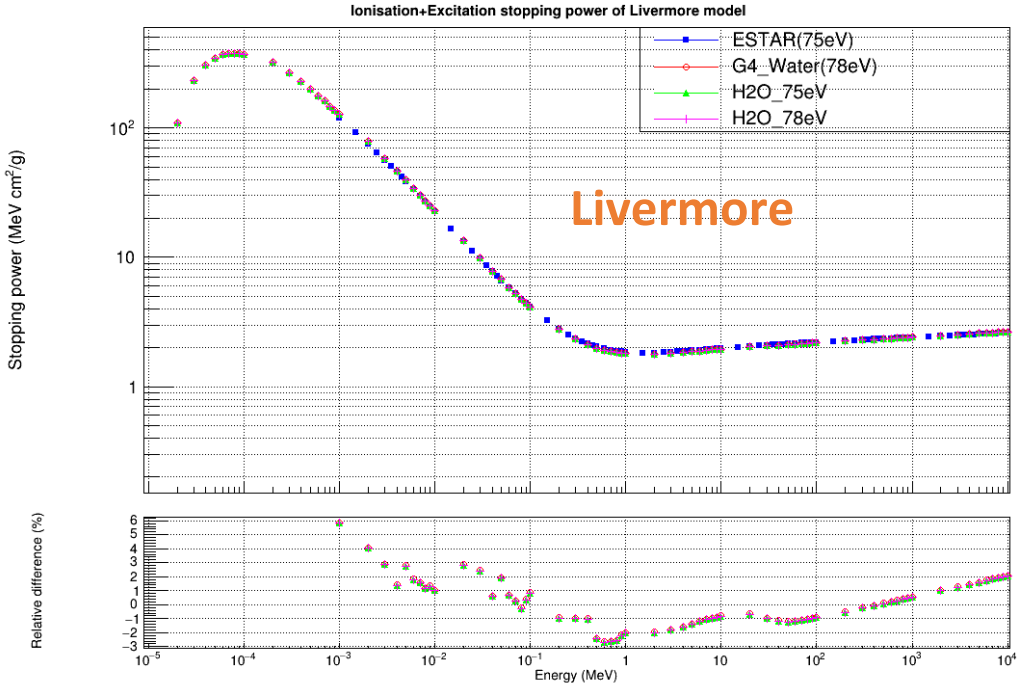
Ionisation+Excitation stopping power of Livermore model
ESTAR(75eV)
G4_Water(78eV)
H2O_75eV
H2O_78eV
Livermore
Stopping power (MeV cm²/g)
Relative difference (%)
Energy (MeV)

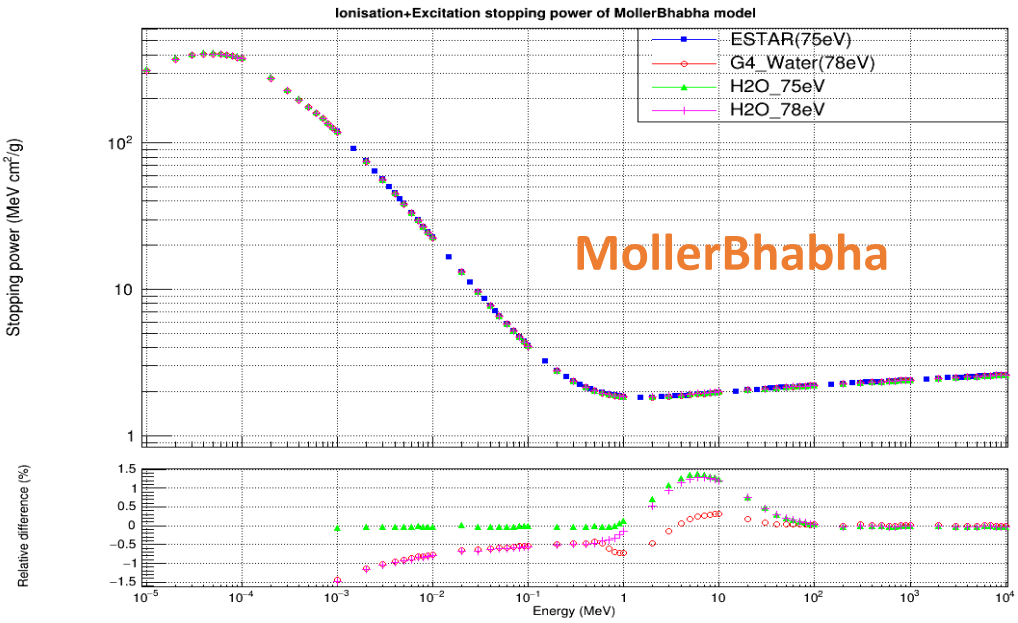

Figure 28. Comparison of stopping power of water with different ionisation potential for three models and ESTAR, calcualted by different models.

6.4. Stopping power comparison in different energy ranges

This comparison was initially meant to decide a more precise energy limit for the use of Livermore ionisation model in ***G4EmLivermorePhysics*** and ***G4EmStandardPhysics_option4*** EM constructors. As mentioned in section 6.31, Livermore ionisation model is no longer used in these two constructors, thus it is useless to refer to this comparison. However, we still keep it in the present technical note for information.

We calculated the relative difference of stopping power of three models compared to ESTAR in three energy ranges, and showed the maximal relative difference as a function of atomic number Z (Figure 29). The three energy ranges are as follows:

- 0.01 - 1 MeV
- 0.01 - 0.3 MeV
- 0.01 - 0.1 MeV

As high energy limit changes, the maximal relative difference for Penelope and MollerBhabha does not change:

- Penelope: 7.23%, Z=97
- MollerBhabha: -2.07%, Z = 94

While Livermore has a variation in different ranges:

- 0.01 - 1 MeV: -11.45%, Z = 1,
- 0.01 - 0.3 MeV: -6.10%, Z = 1,
- 0.01 - 0.1 MeV: -3.24%, Z = 1

In order to clearly see the difference on different models, we plot maximal relative difference separately for different models in Figure 30.

For Livermore model:

- Only hydrogen has a big variation as the high energy limit changes
- For the other elements, the maximal relative difference in the three ranges is always less than 6 %

The maximal value occurs to Z = 97, 7.23% for Penelope and Z = 94, -2.07% for MollerBhabha.

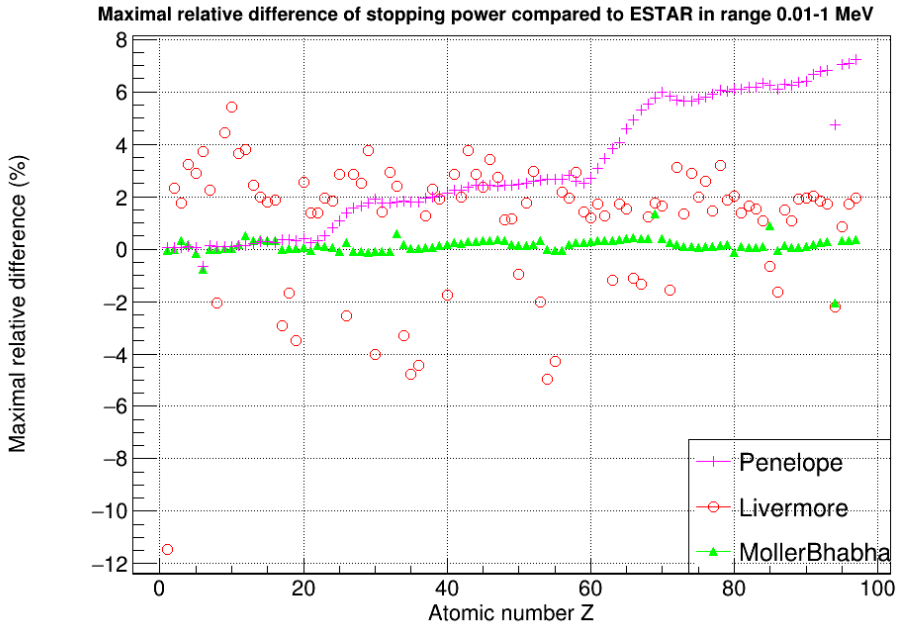

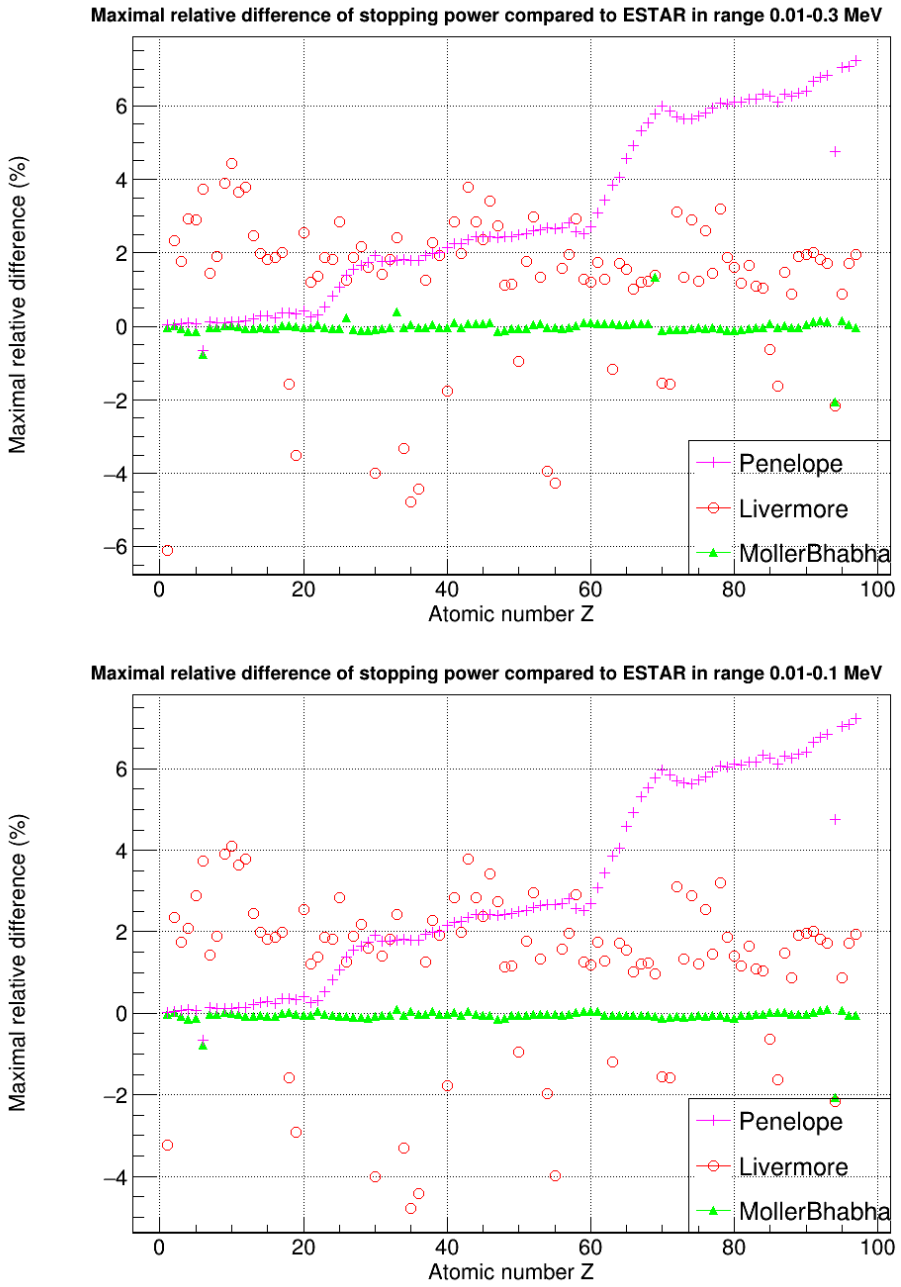

Figure 29. Maximal relative difference of stopping power of three models compared to ESTAR in different energy ranges.

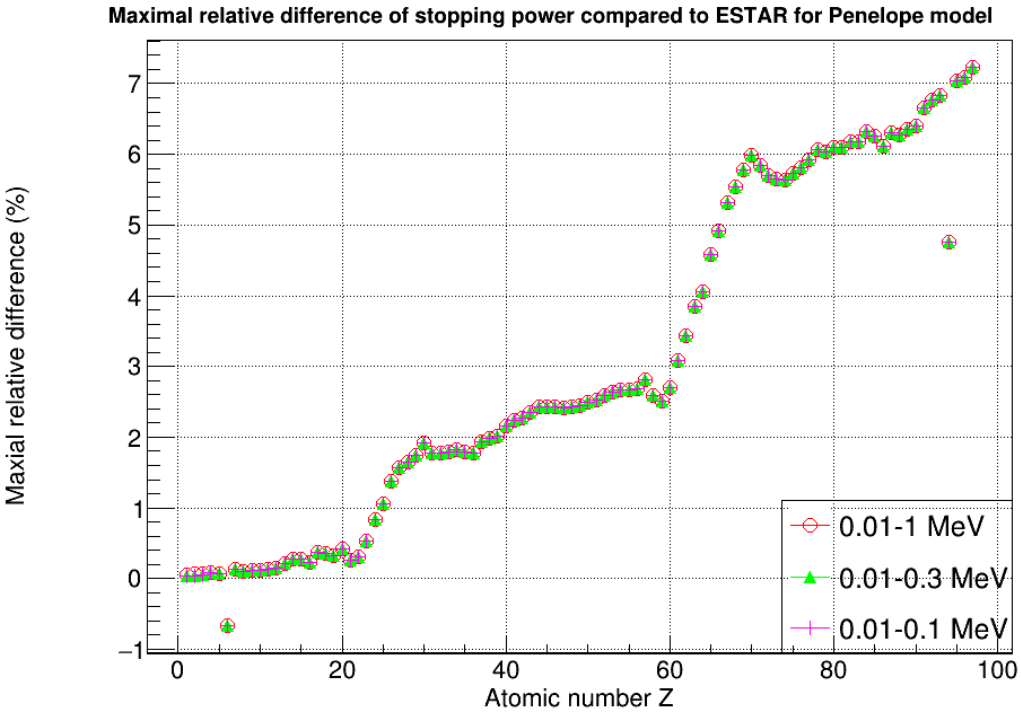
Maximal relative difference of stopping power compared to ESTAR for Penelope model
Maxial relative difference (%)
Atomic number Z
0.01-1 MeV
0.01-0.3 MeV
0.01-0.1 MeV

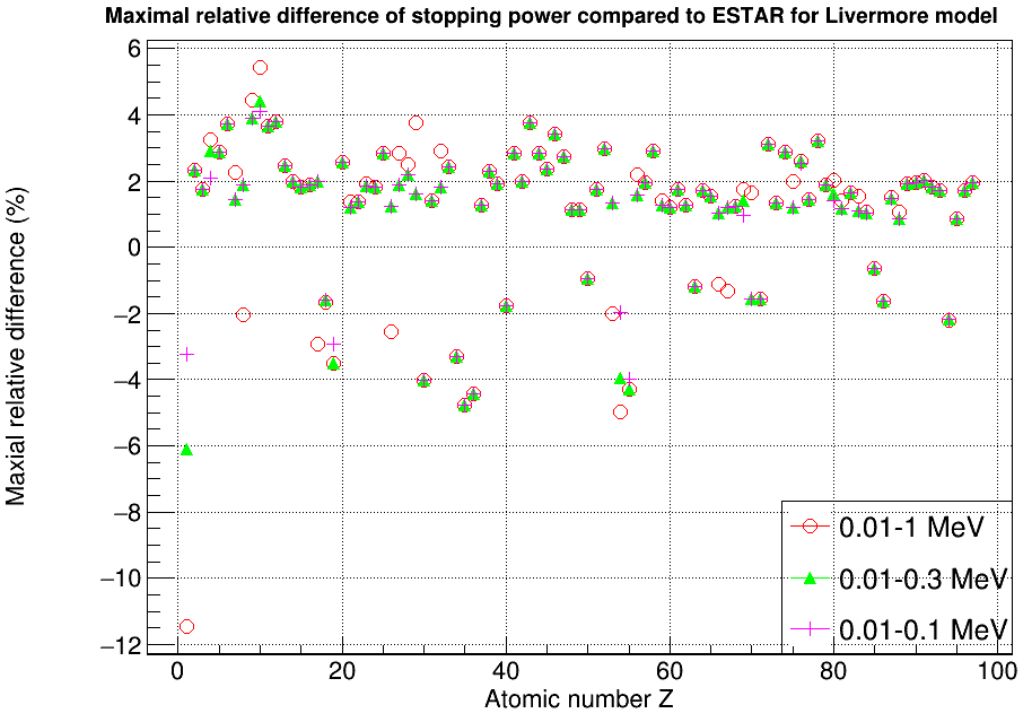
Maximal relative difference of stopping power compared to ESTAR for Livermore model
Maxial relative difference (%)
Atomic number Z
0.01-1 MeV
0.01-0.3 MeV
0.01-0.1 MeV

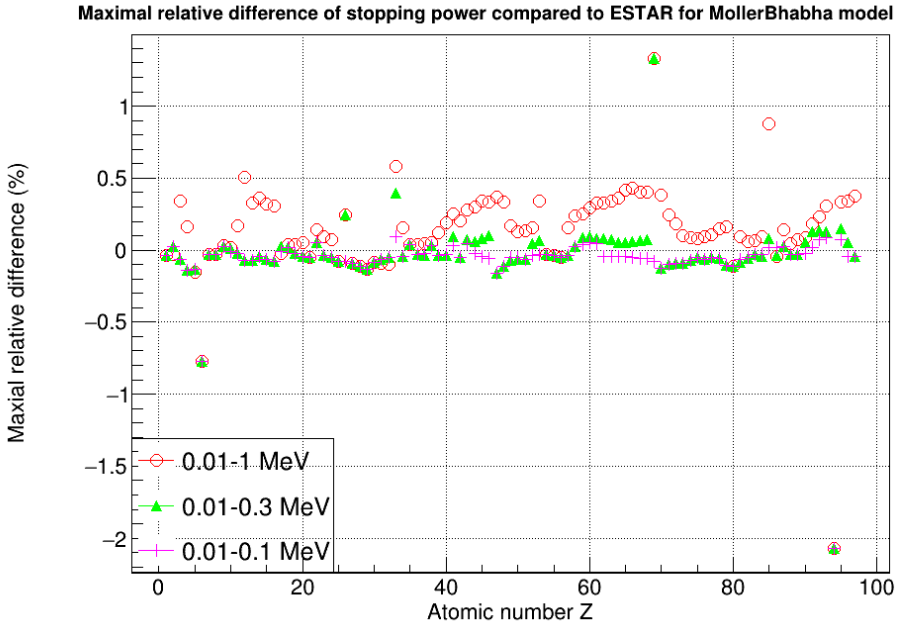

Figure 30. Maximal relative difference of stopping power in different energy ranges for three models compared to ESTAR.

7. Supplementary data

7.1. For analysis of EPICS data

7.1.1. Figures

- Total ionisation cross-sections comparison between EPICS2017 and EPICS2014 for elements Z: 1-100: saved in ***totalCS_2014_2017*** folder;
- Subshell ionisation cross-section comparison between EPICS2017 and EPICS2014 for elements Z: 1-100: saved in ***subshellCS_comparison*** folder and ***subshellCS_comparison/OnePlot***;
- Excitation cross-section comparison between EPICS2017 and EPICS2014 for elements Z: 1-100: saved in ***excitation_cs_comparison*** folder;
- Bremsstrahlung cross-section comparison between EPICS2017 and EPICS2014 for elements Z: 1-100: saved in ***brem_cs_comparison*** folder.

7.1.2. Scripts

- ***generate_ss_cs_2017.C***: read ionisation subshell cross-section from EPICS2017 and generate subshell cross-section files. If it is ended with 2014, it is used for EPICS2014 data;
- ***generate_ss_cs_2017_preliminary.C***: read ionisation subshell cross-section from EPICS2017 and generate subshell cross-section files. The file includes a specific header line, composed of 5 values: first energy value, last energy value, number of points, subshell index and subshell designator;
- ***generate_io_cs_2017.C***: read total ionisation cross-section from EPICS2017 and generate total cross-section files;
- ***compare_SumOfSubShellCSVsTotalCS.C***: verify that tabulated total cross-sections are the sum of tabulated subshell cross-sections using linear interpolation;
- ***compare_ONLY_subshellCS.C***: compare only the subshell cross-section points between EEDL2017 and EEDL2014 for all the elements without taking into account the cross-section points;
- ***compare_ONLY_subshellEnergyPoints.C***: compare only the energy points between EEDL2017 and EEDL2014 for all the elements without taking into account the energy points;
- ***plot_ss_cs.C***: plot the comparison of subshell cross-section between EPICS2017 and EPICS2014;
- ***plot_ss_cs_allSubshellsOnePlot.C***: plot the comparison of subshell cross-section between EPICS2017 and EPICS2014 in one figure;

- ***compare_TotalCS_2014_2017.C***: compare the total ionization cross-section between EPICS2017 and EPICS2014;
- ***generate_br_cs_2017.C***: read bremsstrahlung cross-section from EPICS2017 and generate bremsstrahlung cross-section files;
- ***generate_ex_cs_2017.C***: read excitation cross-section from EPICS2017 and generate excitation cross-section files;
- ***generate_io_sp_2017.C***: read ionisation spectra from EPICS2017 and generate spectra files;
- ***plot_br_cs_2014_2017.C***: plot the comparison of bremsstrahlung cross-section between EPICS2017 and EPICS2014;
- ***plot_ex_cs_2014_2017.C***: plot the comparison of excitation cross-section between EPICS2017 and EPICS2014;
- ***plot_io_sp_2014_2017.C***: plot the comparison of ionisation spectra between EPICS2017 and EPICS2014.

7.2. For cross-section and stopping power analysis

All the data are saved under ***CrossSection_StoppingPower_ComparisonStudy***

7.2.1. For cross-section study

- The data are saved in ***CrossSection_StoppingPower_ComparisonStudy/Cross_section_study***
- The figures are saved in ***CrossSection_StoppingPower_ComparisonStudy/Cross_section_study/plots***

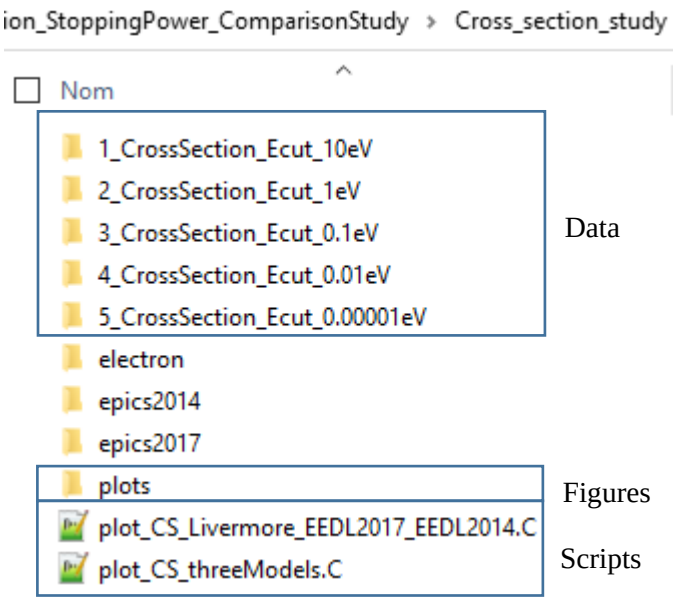

Figure 31. Data and figures paths for cross-section study.

7.2.1. For stopping power study

- The data are saved in ***CrossSection_StoppingPower_ComparisonStudy/Stopping_power_study***
- The figures are saved in ***CrossSection_StoppingPower_ComparisonStudy/Stopping_power_study/plots***

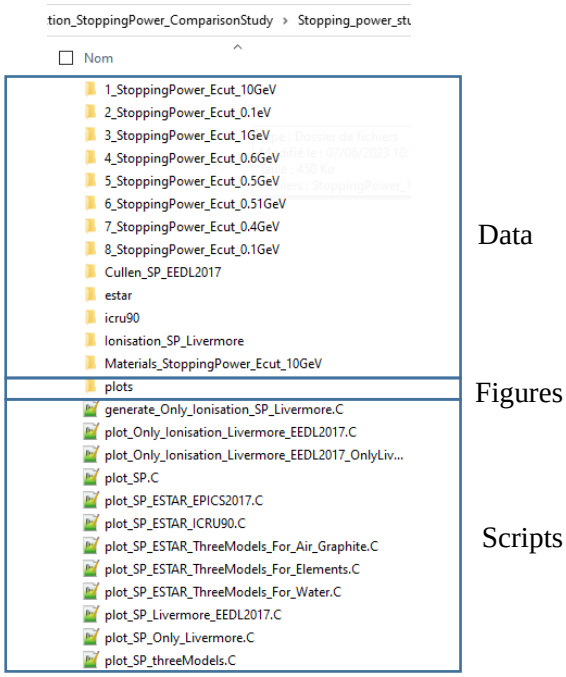

Figure 32. Data and figures paths for stopping power study.

Reference

[1] Li Z. Implementation of the EPICS2017 electron-photon database in Geant4: developments and applications: Université de Bordeaux (Ph.D Thesis); 2023.

[2] Cullen DE. A Survey of Electron Cross Section Data for use in EPICS2017. IAEA-NDS-226. 2017. https://www-nds.iaea.org/publications/nds/iaea-nds-0226/.

[3] Deslattes RD, Kessler EG, Indelicato P, de Billy L, Lindroth E, Anton J. X-ray transition energies: new approach to a comprehensive evaluation. Rev Mod Phys. 2003;75(1):35-99. https://doi.org/10.1103/RevModPhys.75.35.

[4] Cullen DE. EPICS2017: April 2019 status report. IAEA-NDS-228. 2019. https://www-nds.iaea.org/epics/DOCUMENTS/2019-EPICS2017-Status.pdf.

[5] Cullen DE. A survey of photon cross section data for use in EPICS2017. IAEA-NDS-225. 2018. https://www-nds.iaea.org/publications/nds/iaea-nds-0225/.

[6] Cullen DE. A Survey of Atomic Binding Energies for use in EPICS2017. IAEA-NDS-224. 2018. https://www-nds.iaea.org/publications/nds/iaea-nds-0224/.

[7] Apostolakis J, Wright DH, collaboration G. An Overview of the Geant4 Toolkit. AIP Conf Proc. 2007;896(1):1-10. https://doi.org/10.1063/1.2720452.

[8] Apostolakis J, Asai M, Bogdanov AG, Burkhardt H, Cosmo G, Elles S, et al. Geometry and physics of the Geant4 toolkit for high and medium energy applications. Radiat Phys Chem. 2009;78(10):859-73. https://doi.org/10.1016/j.radphyschem.2009.04.026.

[9] Geant4 collaboration. Physics reference manual. 2020;9(0). https://geant4-userdoc.web.cern.ch/UsersGuides/PhysicsReferenceManual/fo/PhysicsReferenceManual.pdf.

[10] Perkins S, Cullen D, Seltzer S. Tables and graphs of electron-interaction cross-sections from 10 eV to 100 GeV derived from the LLNL evaluated electron data library (EEDL), Z= 1-100. UCRL-50400. 1991;31:21-4. https://doi.org/10.2172/5691165.

[11] Berger MJ. ESTAR, PSTAR, and ASTAR: Computer programs for calculating stopping-power and range tables for electrons, protons, and helium ions. 1992. https://dx.doi.org/10.18434/T4NC7P.

[12] Seltzer S, Fernandez-Varea J, Andreo P, Bergstrom P, Burns D, Krajcar Bronić I, et al. Key data for ionizing-radiation dosimetry: measurement standards and applications, ICRU Report 90. 2016. https://www.icru.org/report/icru-report-90-key-data-for-ionizing-radiation-dosimetry-measurement-standards-and-applications/.